UNITED NATIONS EDUCATIONAL, SCIENTIFIC AND CULTURAL ORGANIZATION
INTERNATIONAL CENTRE FOR THEORETICAL PHYSICS
I.C.T.P., P.O. BOX 586, 34100 TRIESTE, ITALY, CABLE: CENTRATOM TRIESTE

H4.SMR/773-7

College on Medical Physics:
Radiation Protection and Imaging Techniques

5 - 23 September 1994

Principles of Imaging Techniques in Nuclear Medicine

and

Radioisotopes and Equipment in Nuclear Medicine

Sören Mattsson

Dept. of Radiation Physics
Lund University
Malmö
Sweden

MAIN BUILDING STRADA COSTIERA, 11 TEL. 22401 TELEFAX 224163 TELEX 460392 ADRIATICO GUEST HOUSE VIA GRIGNANO, 9 TEL. 224241 TELEFAX 224531 TELEX 460449
MICROPROCESSOR LAB. VIA BEIRUT, 31 TEL. 224471 TELEFAX 224600 TELEX 460392 GALILEO GUEST HOUSE VIA BEIRUT, 7 TEL. 22401 TELEFAX 2240310 TELEX 460392

In Vivo Nuclear Medicine

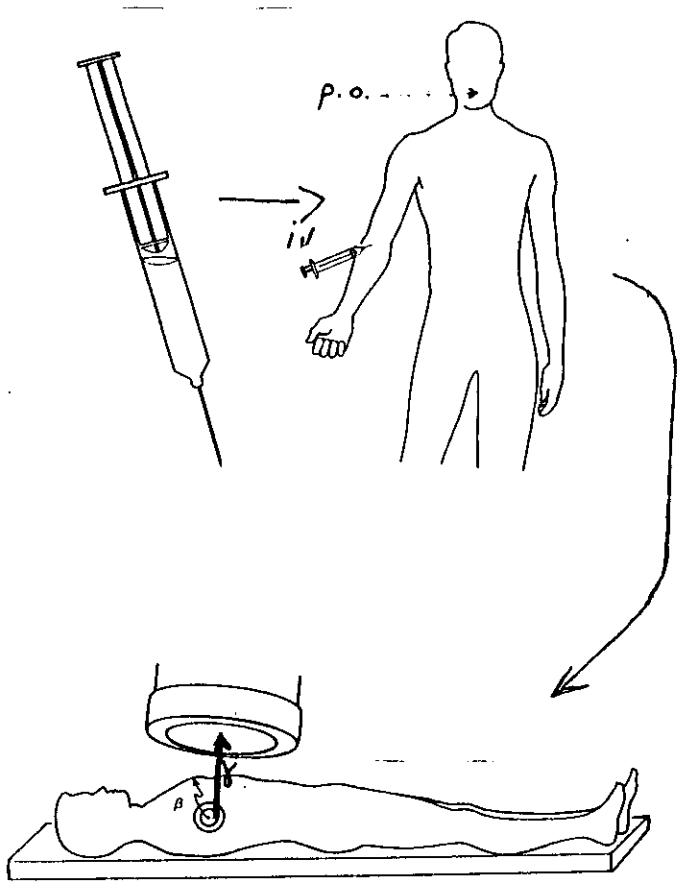

Iodine's specificity for thyroid tissue was quickly adapted to nuclear medicine, first in metabolic studies in animals and subsequently as a radiopharmaceutical for diagnostic studies and for therapy. Photo made by Joseph Hamilton around 1940 is one of first showing radioiodine uptake being recorded by a Geiger counter.

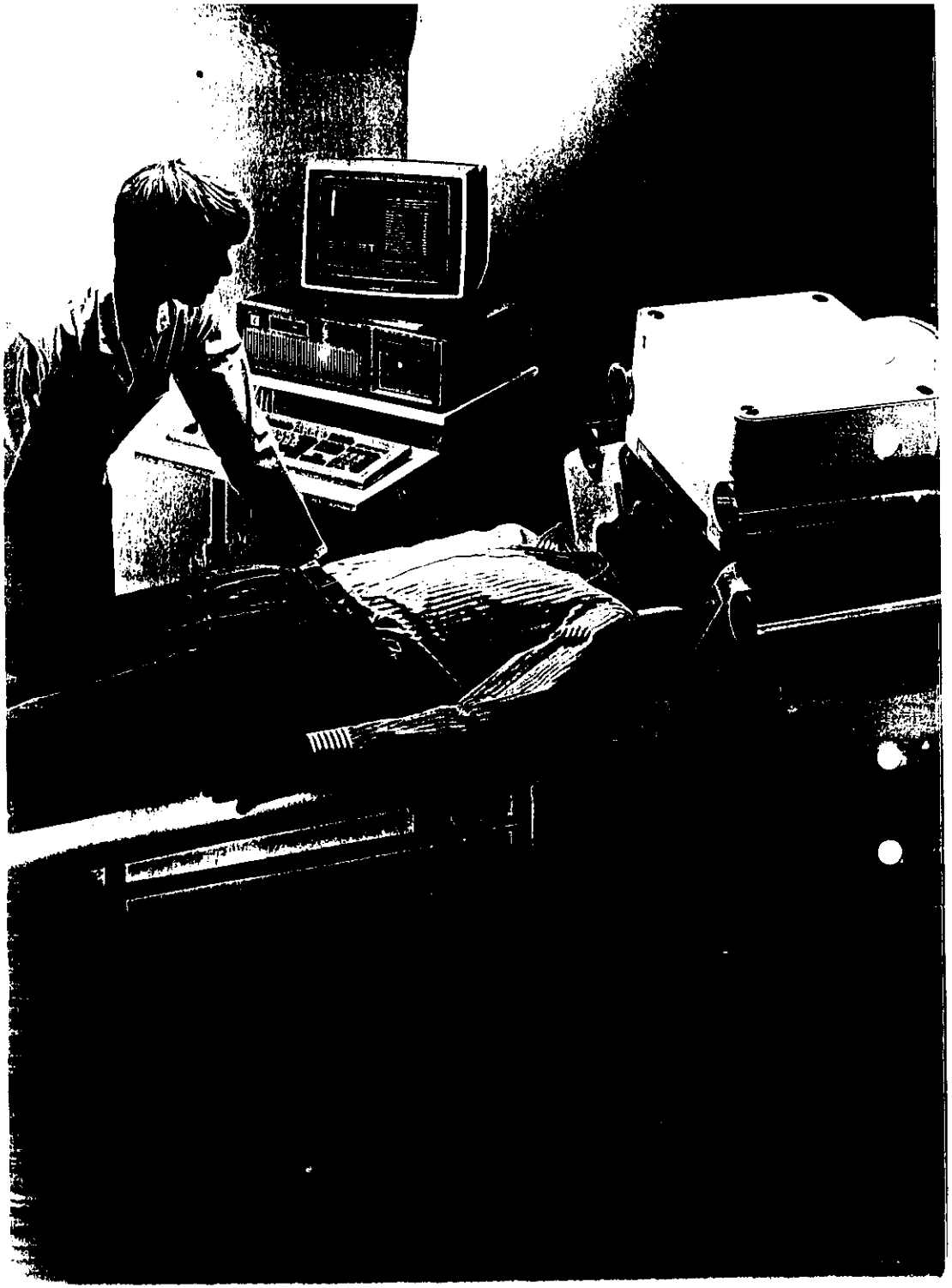

Upatial resolution

Nuclear medicine

Gammacamera	≈ 10 mm	140 keV
SPECT	10 - 20 mm	"
" center	10-12 mm	"
(Cylindrical GC	6-7 mm)	"
PET	5 mm	511 keV

X-ray diagnostics

Normal X-rays	< 0,1 mm
CT	0,2 mm

What is special with nuclear medicine ?

The sensitivity !

nmol/ml

10^{-12}

ppb

This has to be used

Detector intrinsic efficiency 85%
Geometrical efficiency 0.02%

Detection should be improved !

Detector geometry 0.02%

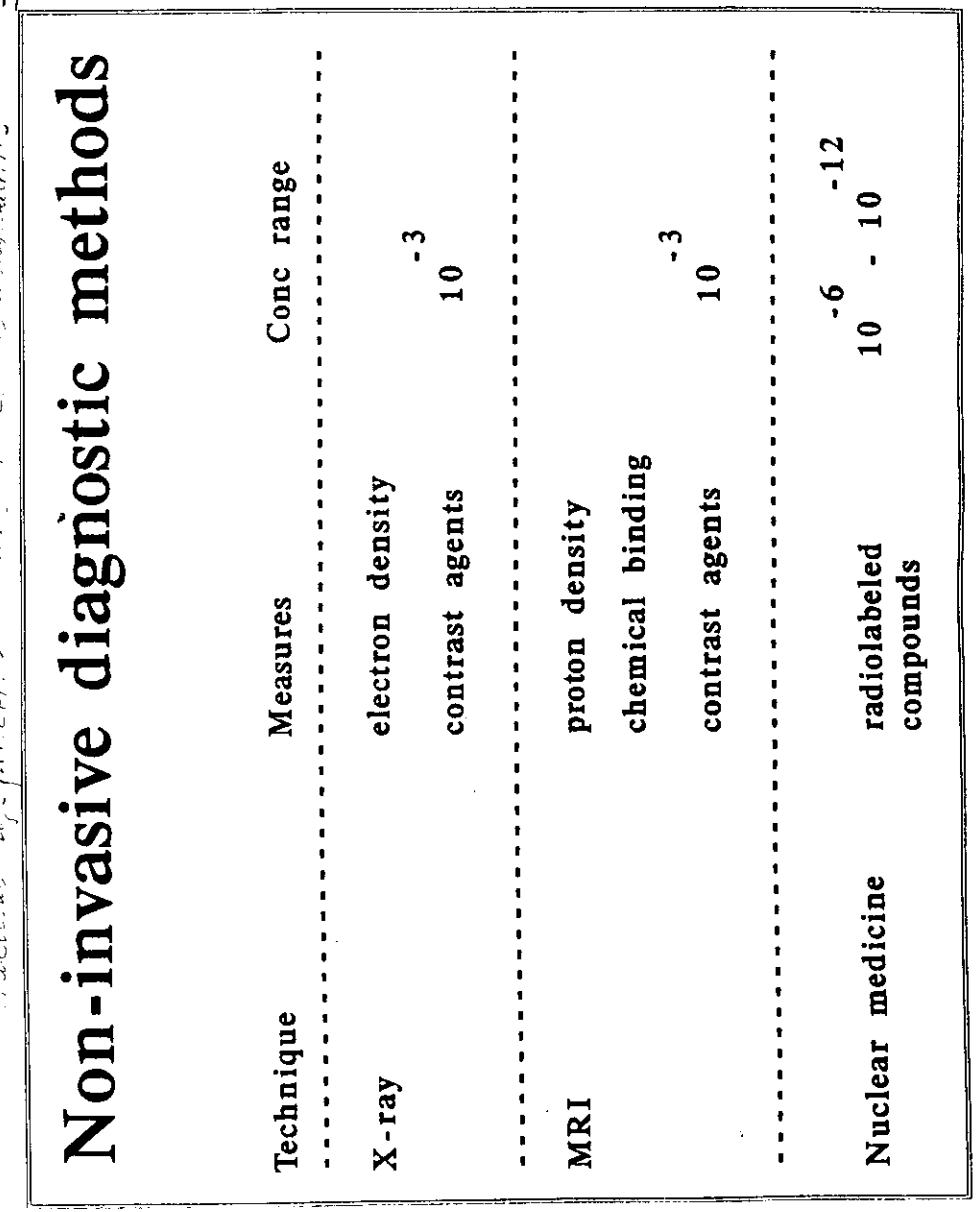

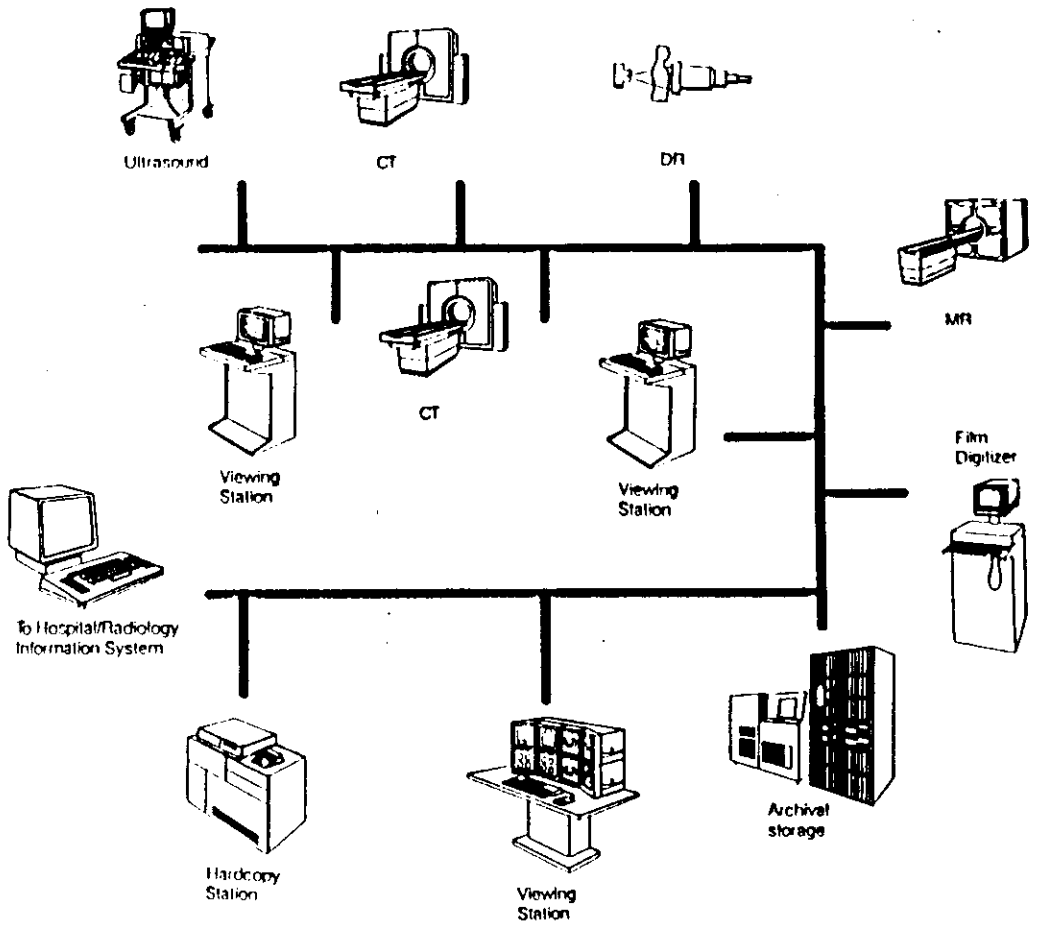

PACS

Picture Archiving and Communication

Diagnostic nuclear medicine in Sweden
1985-87 Ca 110 000 investigations/year

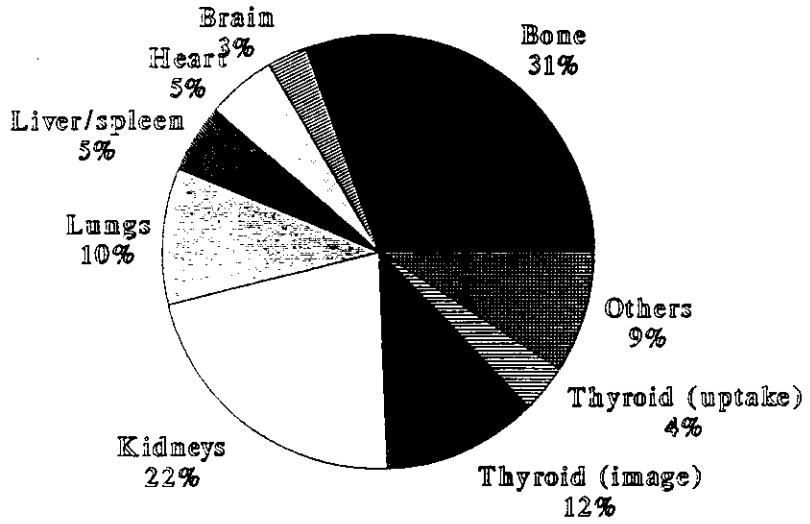

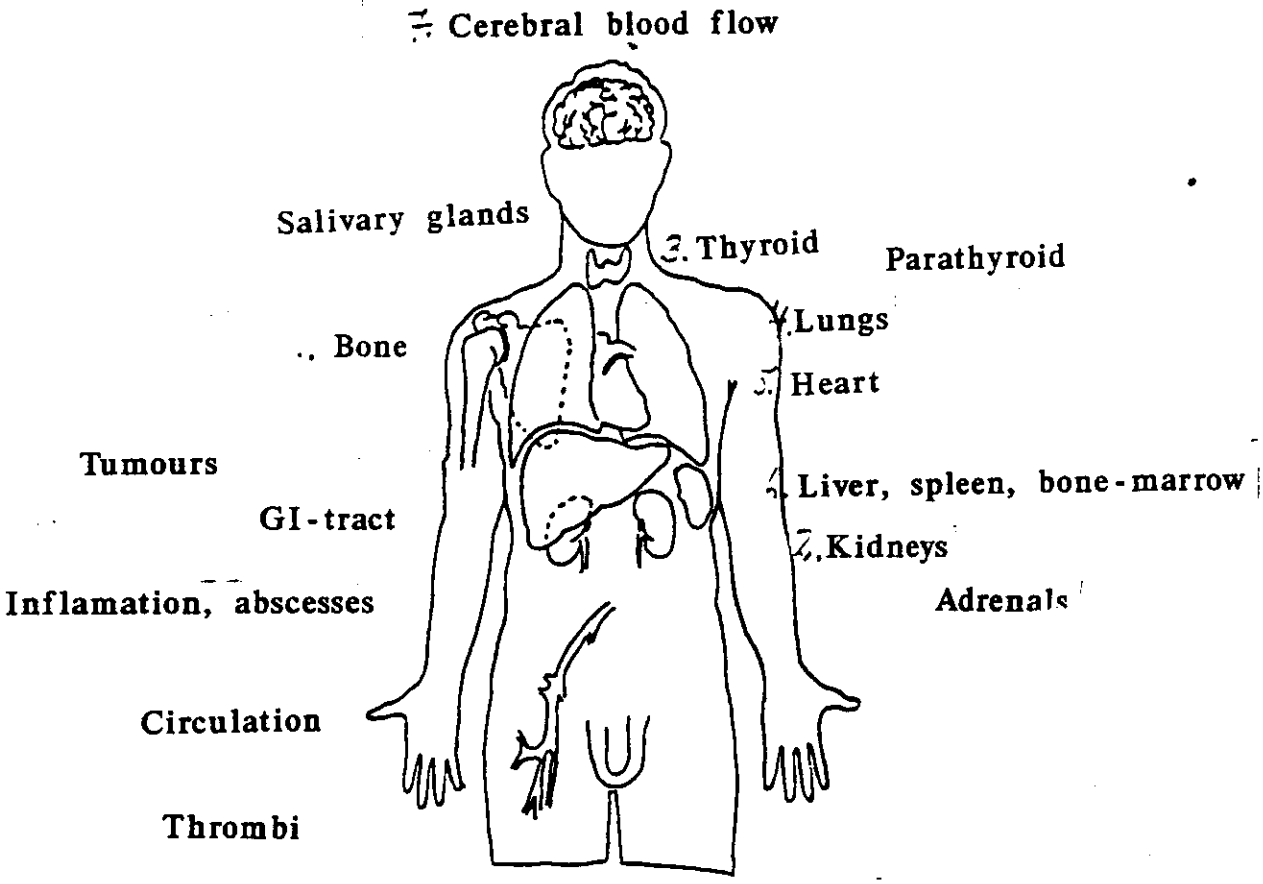

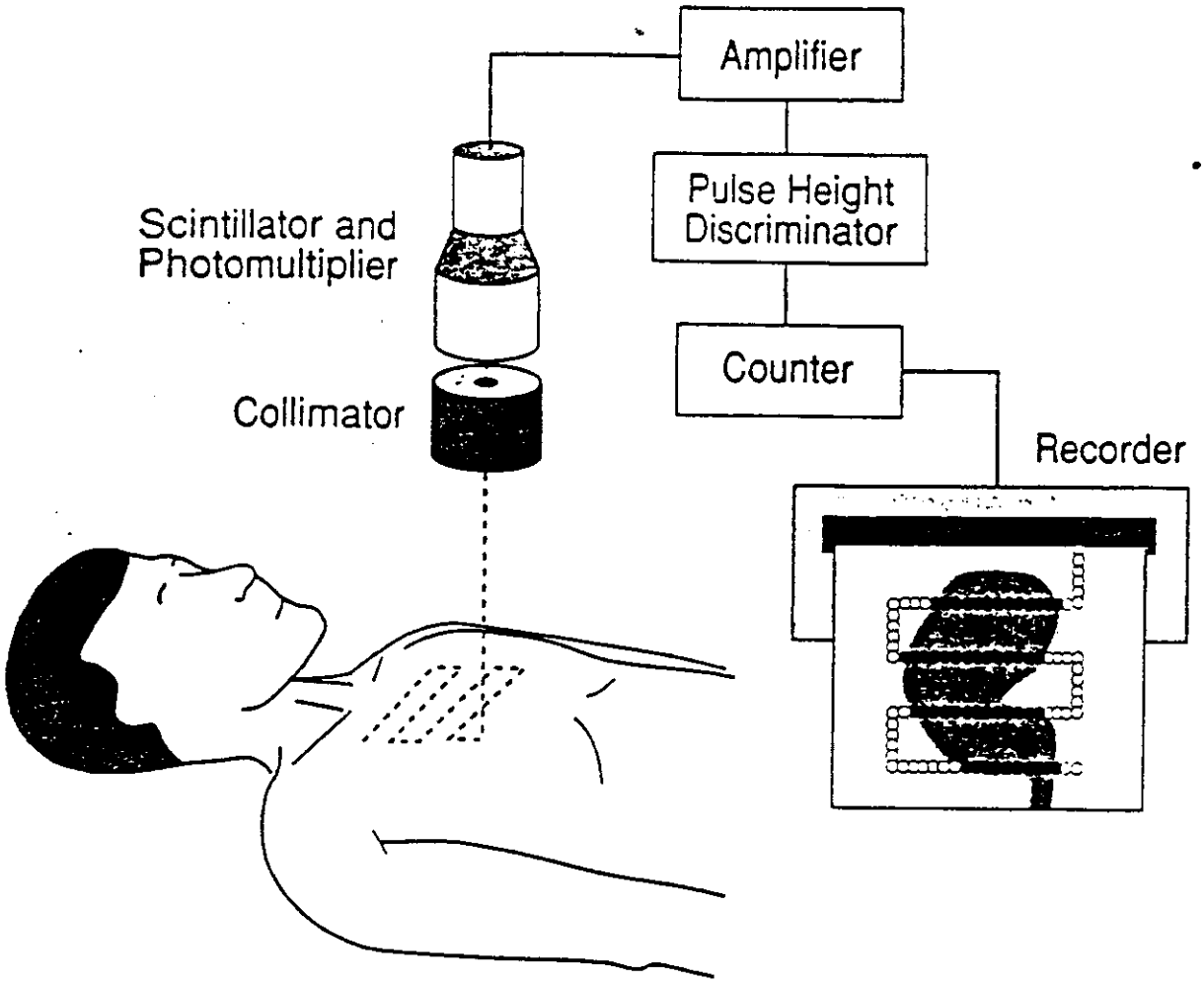

Instrumentation

Gamma - camera

Rotating gamma - camera, SPECT

Positron camera, PET

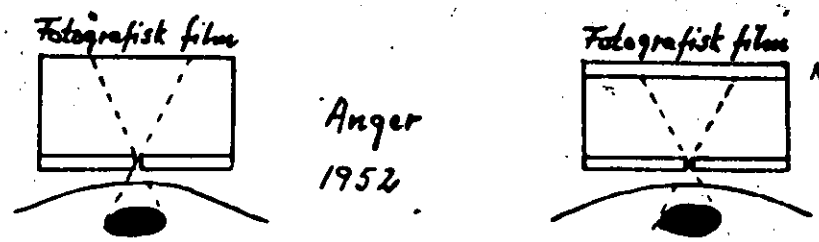

Anger
1952

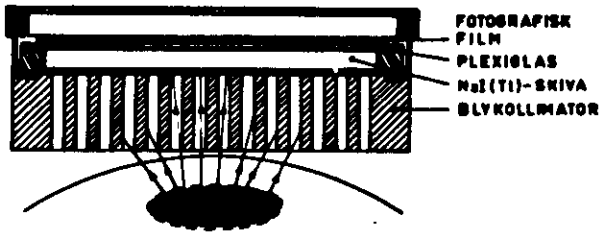

Johansson och Skanse, 1953

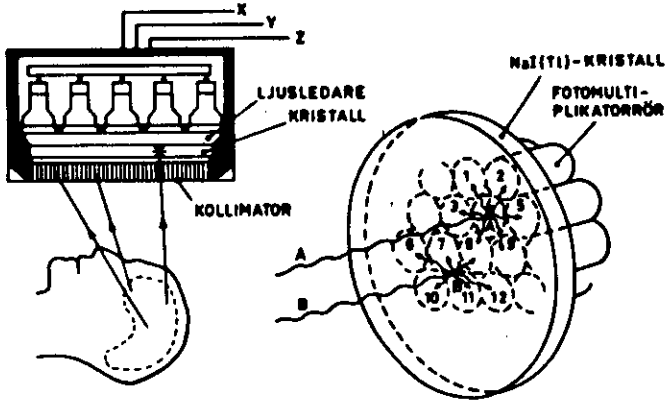

Anger, 1956
(7 PM-rör)

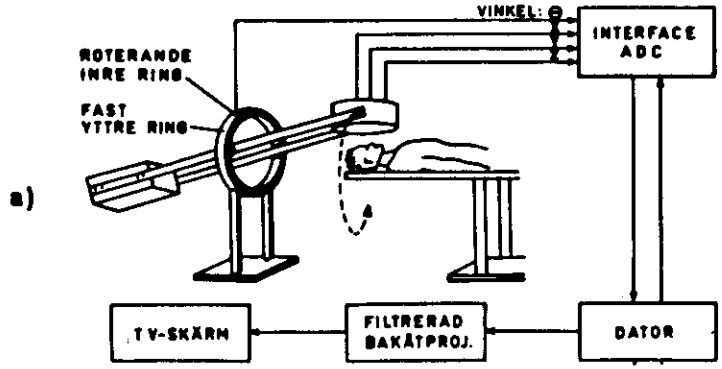

SPECT
Kuhl, 1963
Budinger m.fl. 1974
Larsson Ericsson 1978

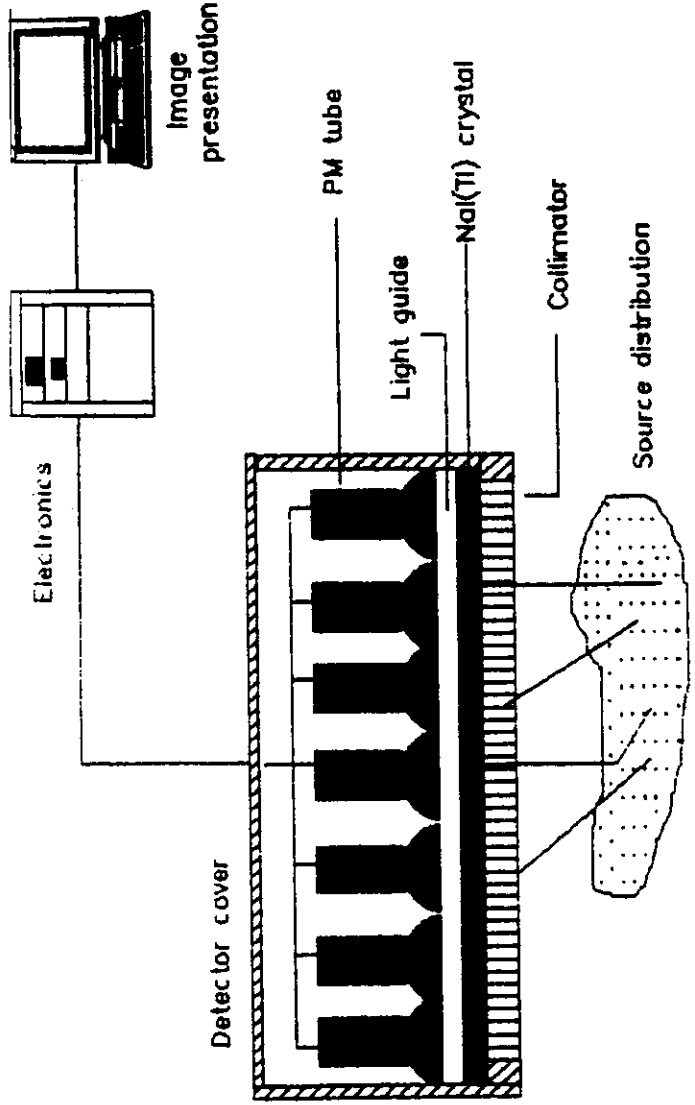

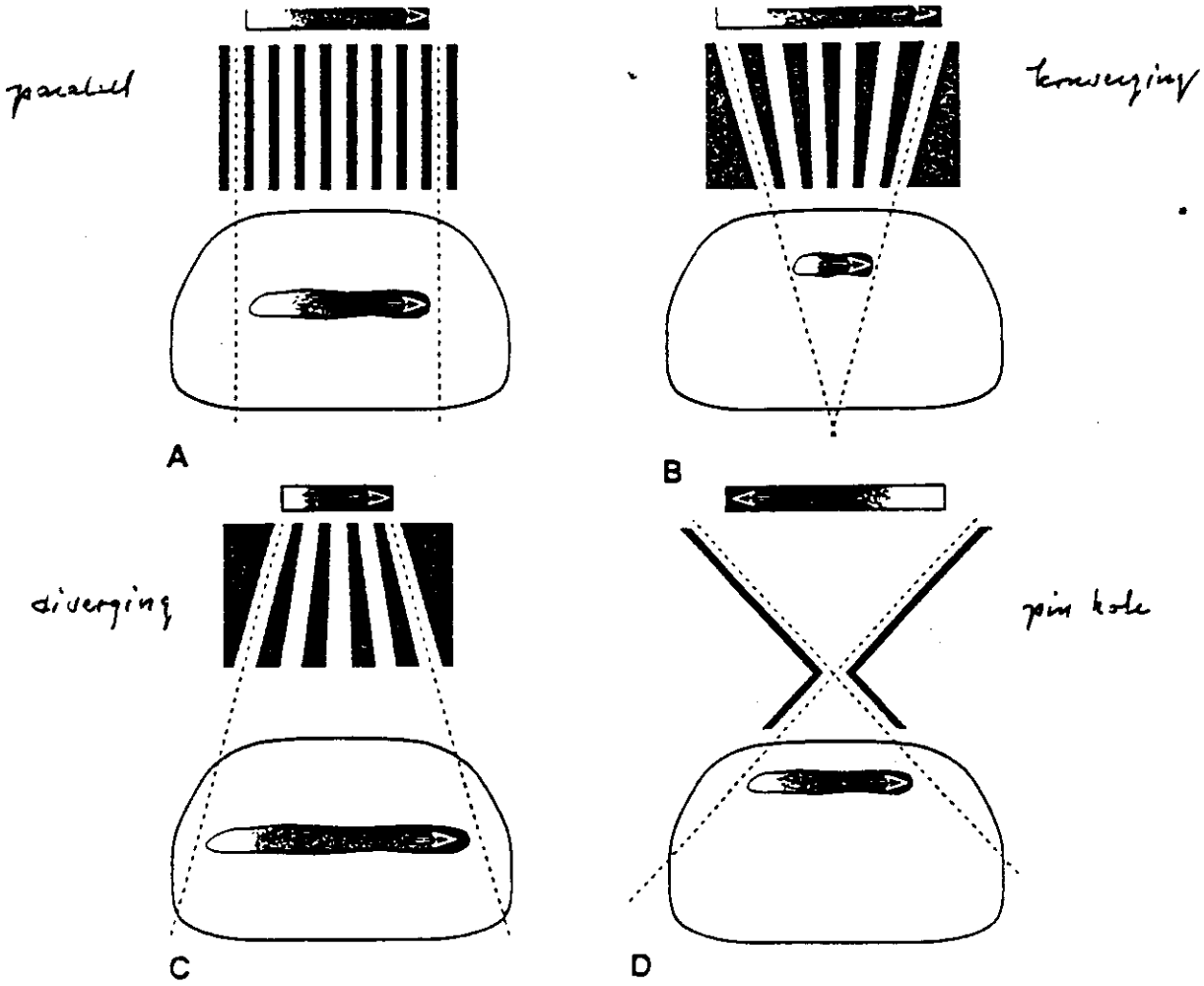

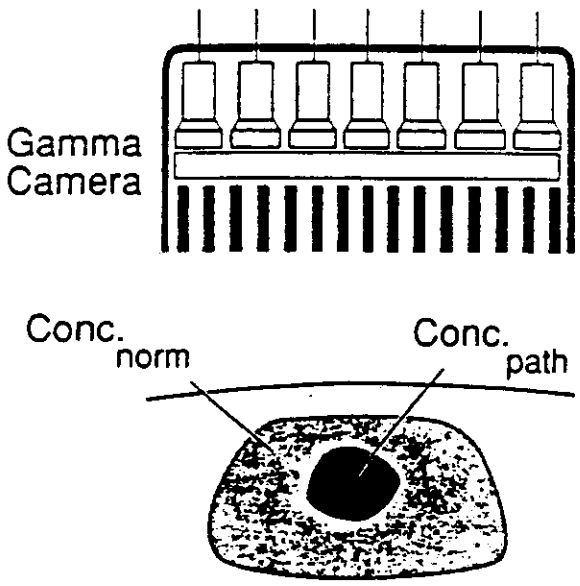

Subject Contrast

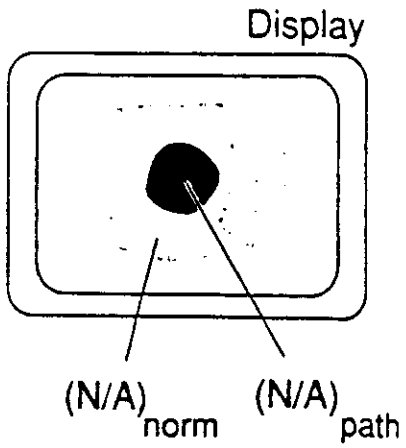

Image Contrast

Parallell hole collimator

Low Energy General Purpose (LEGP)
hν < 150 keV
18000 holes, Φ = 2,3 mm, septa 0,3 mm

Low Energy High Resolution (LEHR)
hν < 150 keV
30 000 holes, Φ = 1,8 mm, septa 0,3 mm

Low Energy High Sensitivity (LEHS)
hν < 150 keV
9000 holes, Φ = 3,4 mm, septa 0,3 mm

Medium Energy High Sensitivity (MEHS)
hν < 350 - 400 keV
6000 holes, Φ = 3,4 mm septa 1,4 mm

High Energy High Sensitivity (HEHS)
hν > 350 keV
1000 holes septa very thick

System resolution

$$R_t = \sqrt{R_i^2 + R_k^2}$$

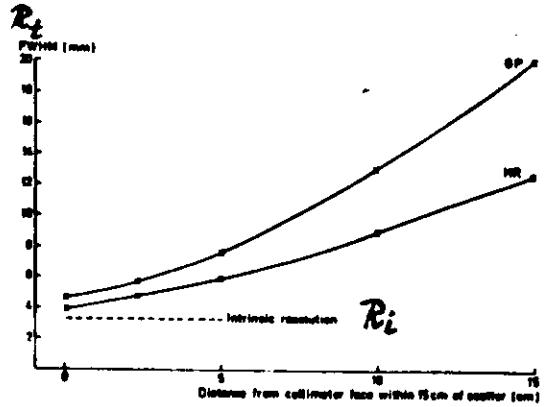

Figure 1. Intrinsic resolution on the crystal face plus the variation in system resolution with depth with both the general purpose (GP) and high resolution (HR) collimators.

Systemets totala upplösningsförmåga beskrivs av kollimatorns egenskaper

Intrinsic resolution

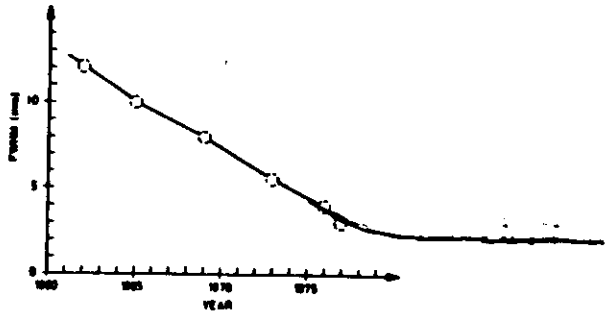

FIG. 1. The change in resolution performance for the past 15 years. Resolution is given as the full width half maximum at 140 keV for the commercially available cameras with the best spatial resolution at that time. These figures are approximate.

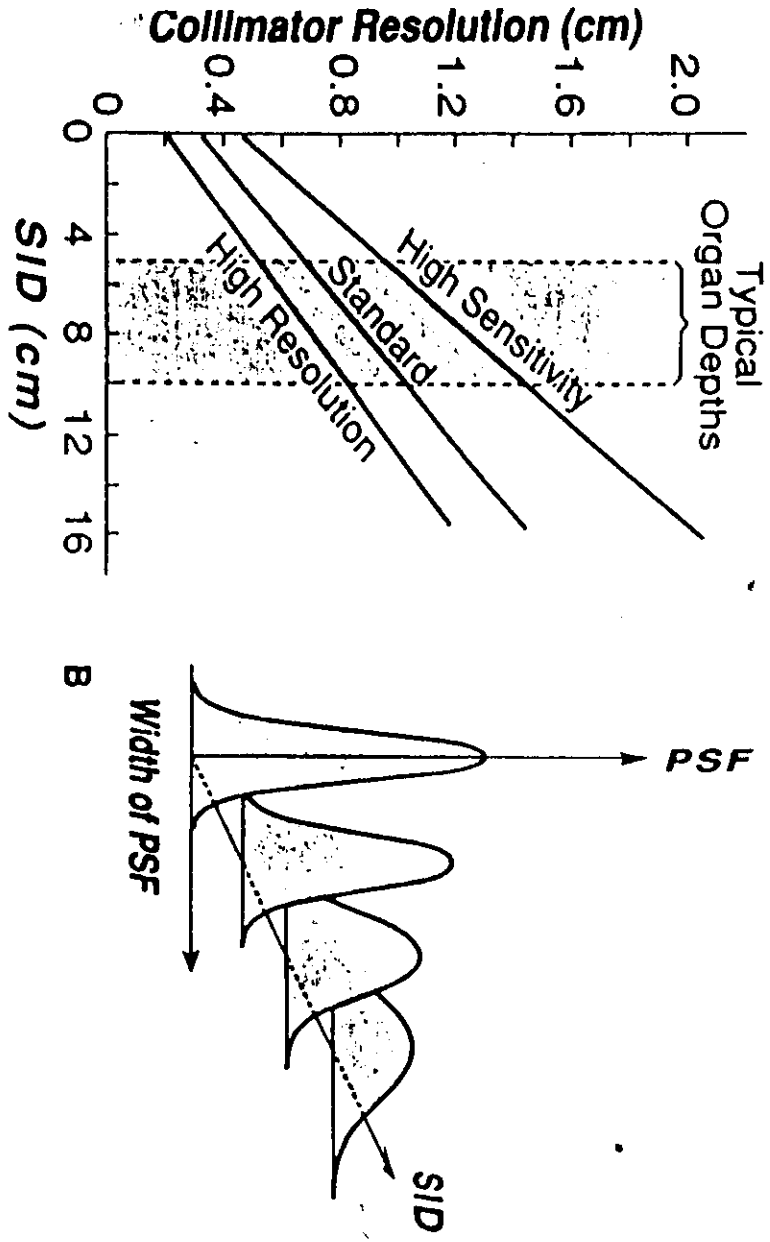

Spatial resolution of gamma cameras (FWHM in CFOV)

State-of-the-art

Detector itself *"Intrinsic resolution"*	3-4 mm
Detector with LEHR-collimator; source at 10 cm *"System resolution"*	7.8 mm (no scatterer) 8.6 mm (with scatterer)
Tomography with LEHR *"Reconstructed system resolution"*	8-10 mm (central) 8-10 mm (radial) 6-8 mm (tangential)

SPECT

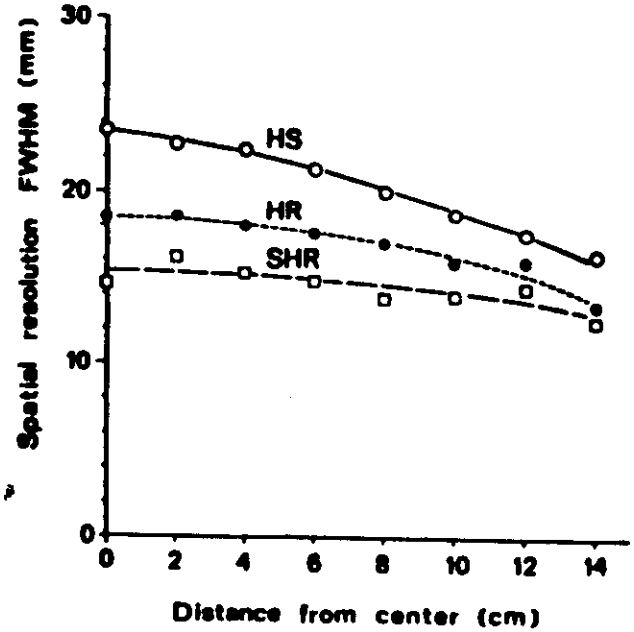

Fig. 44. Spatial resolution (FWHM) as a function of the distance from center of a transverse section using the HS-collimator (—), the HR-collimator (•---•) and the SHR-collimator (▫--▫). Source: $^{99}Tc^{m}$.

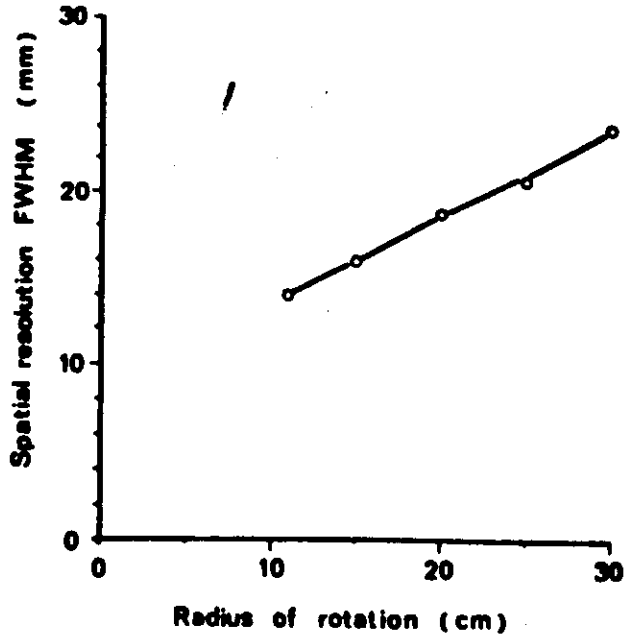

Fig. 46. Spatial resolution (FWHM) at the center of a transverse section as a function of the radius of rotation. Source: $^{99}Tc^{m}$.

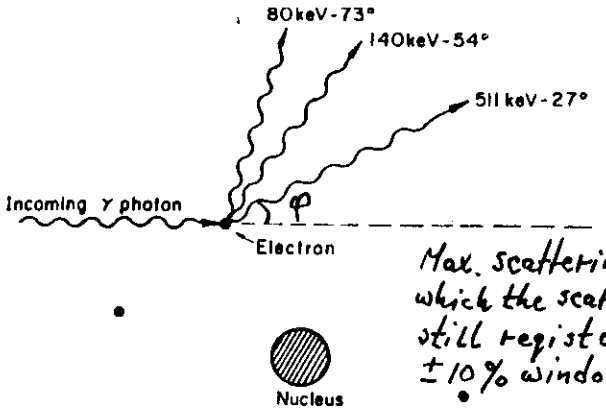

Max. scattering angle φ for which the scattered photon is still registered in a ±10% window

Fig. 3. The angular distribution of photons is dependent on the energy of the incoming photon before scattering.

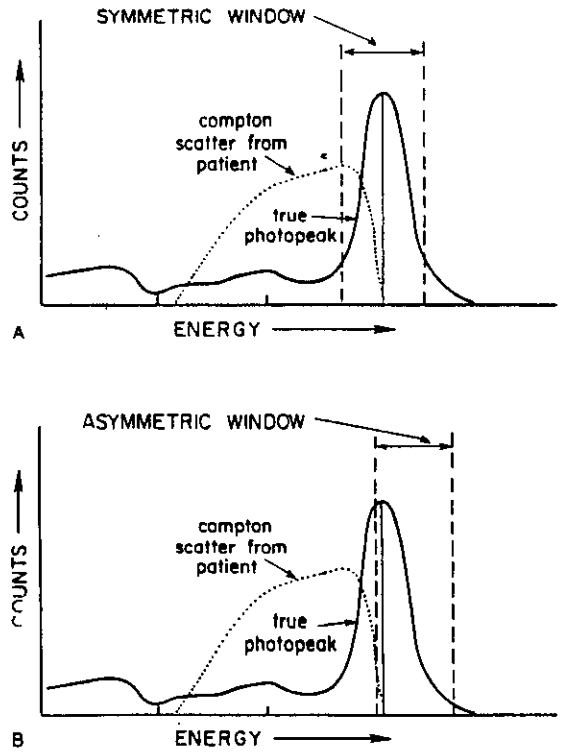

Figure 2–5. Use of a symmetric window (A) allows some of the Compton scatter to be counted and displayed. Theoretically, use of an asymmetric window (B) obviates this problem.

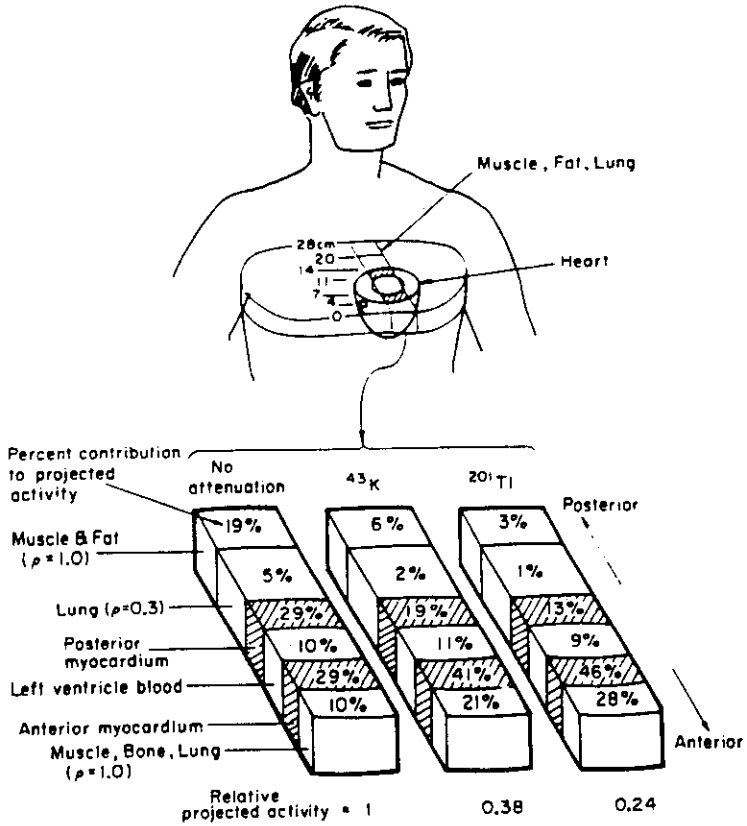

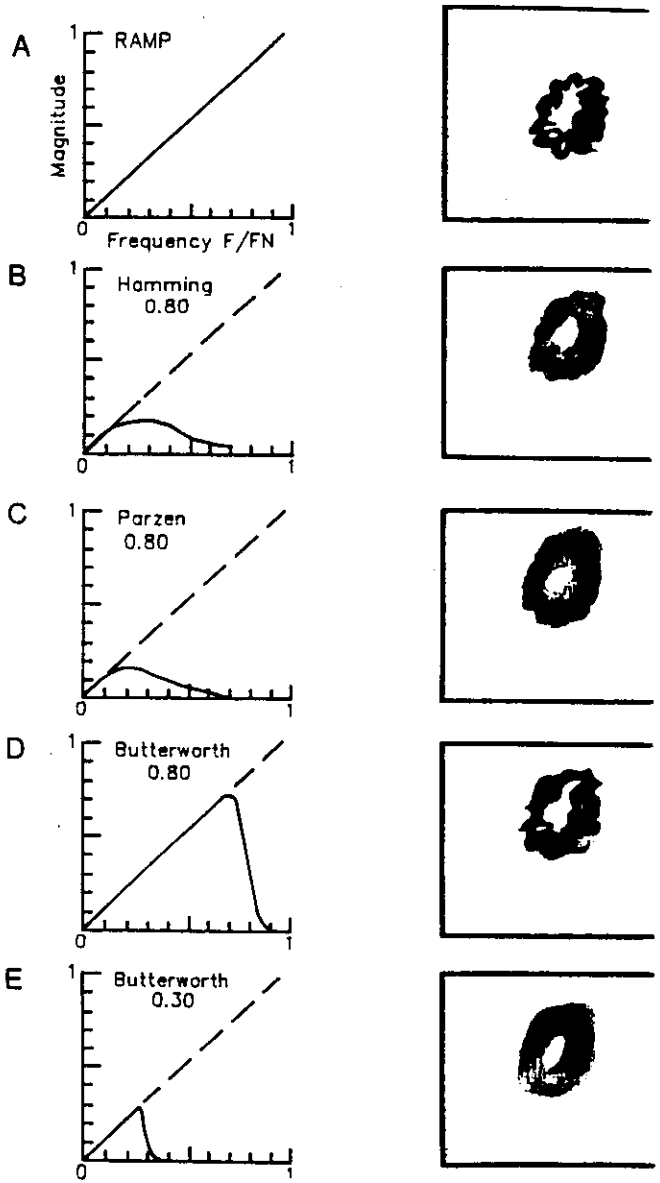

gure 4–2. (A) A pure ramp filter displayed in frequency space is so called because the value of the filter increases as the spatial frequency increases. The filter is usually applied to the back projection process to attenuate the low frequencies and thus to sharpen edges blurred during the process. (B to E) Additional filters are frequently needed if the images obtained are degraded by the presence of high-frequency noise. In these cases, a window may be applied to the ramp filter, which is set to "cutoff" at a certain frequency (shown here from 0.3 to 0.8). The final reconstruction filters are a product of the ramp filter and the window function. In general, a cutoff value that is too low produces oversmoothed data, which may obscure lesions. A cutoff value that is too high can produce noisy images that have a patchy appearance. The selection of a filter for image processing should consider both the frequency context of the noise in the image as well as the inherent frequency context of the organ being imaged. (Fischer KC: Qualitative SPECT thallium imaging: Technical and clinical applications. In Guiberteau M: Nuclear Cardiovascular Imaging: Current Clinical Practice. New York, Churchill Livingstone, 1990.)

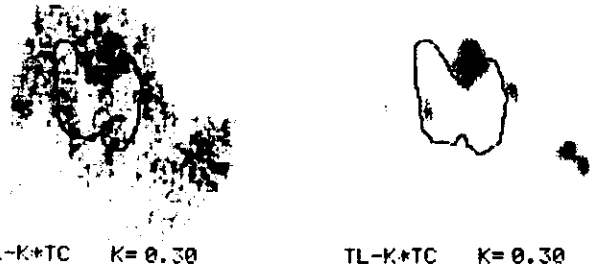

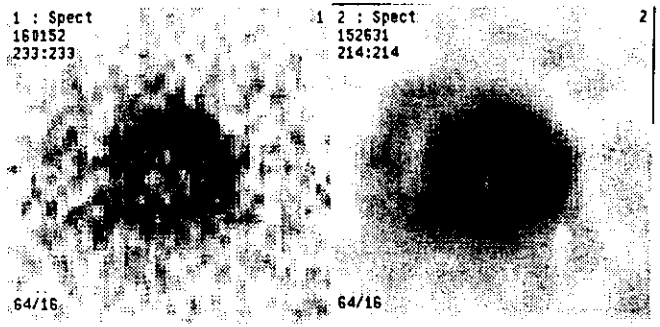

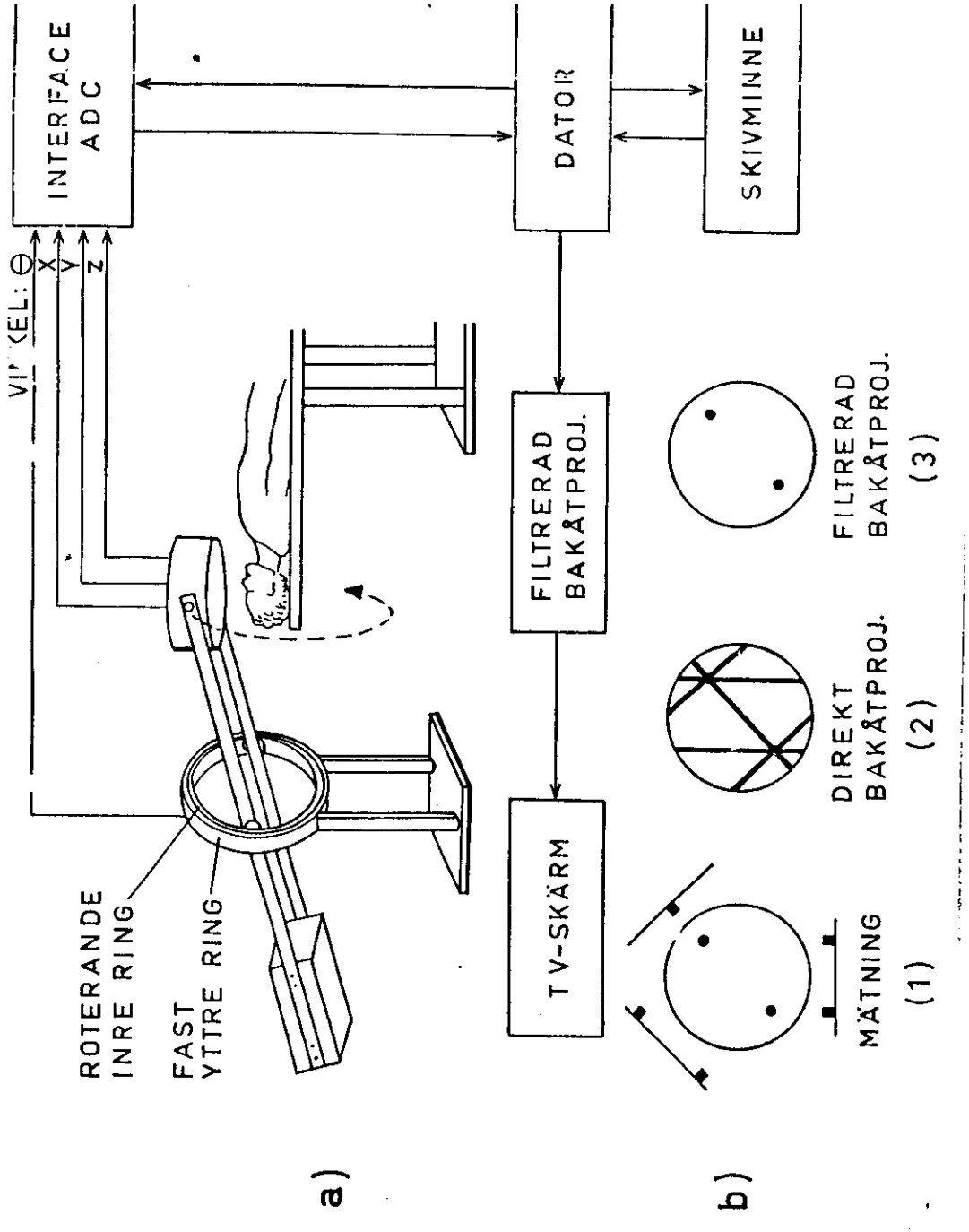

Tomography with gamma camera

2D - Reconstruction Methods

A. Back projection

B. Analytical methods

1. Filtered back projection
2. Back projection filtering
3. Two-dimensional Fourier reconstruction

C. Iterative methods

1. Algebraic reconstruction
2. Simultaneous technique
3. Least-square technique

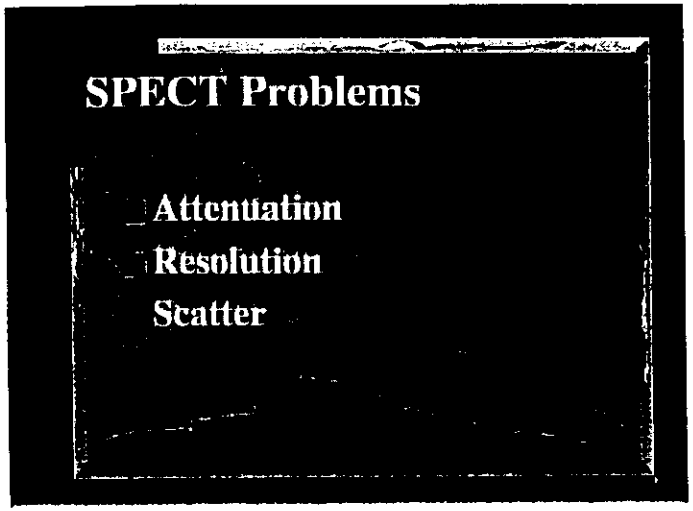

Some attenuation correction methods

*A. **Pre-processing methods*** (Sorensen 74, Larsson 80)
- Geometrical or arithmetrical mean of opposite projections
- Assume constant attenuation coefficient
- Assume uniform activity distribution

*B. **Post-processing methods*** (Chang 78, Larsson 80, Axelsson 87, ...)
- Calculate correction factors from a first-order SPECT image
- Corrections applied to projections or SPECT image
- Allow for uniform or nonuniform attenuation
- Takes source distribution into account
- Can be made iterative

*C. **Intrinsic correction methods***
- Part of an iterative reconstruction method
- Allow for uniform/nonuniform attenuation
- Can also include scatter and collimator response corrections

Attenuation correction
Preprocessing "

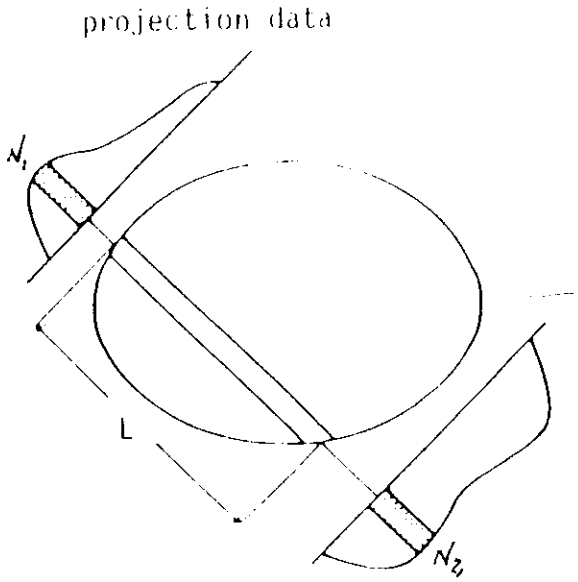

$$\frac{N_1 + N_2}{2} \cdot \frac{\mu L}{1 - e^{-\mu L}}$$

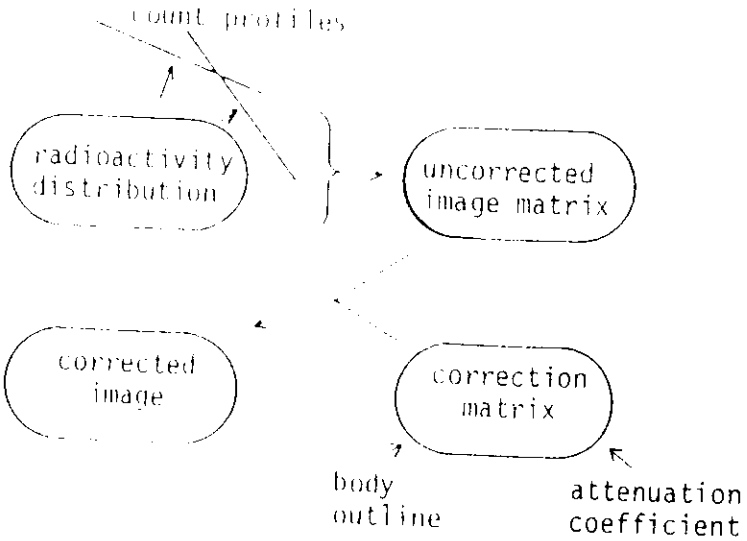

Methods for non-homogeneous attenuation correction

A. Transmission SPECT measurements
- Uncollimated flood- or line source and parallel hole collimator
- Collimated flood- or line source and parallel hole collimator
- Line source and fan beam collimator
- Line source and slant hole collimator

B. Computed tomography
- Superior resolution compared to transmission SPECT
- Require an additional study
- Potential problems in patient realignment

C. Compton scatter acquisition
- Acquisition of Compton scatter images
- Sophisticated segmentation methods to outline body and lungs
- Lungs and tissue are assigned fixed attenuation values

Body outline

A. Elliptical outline from point source measurements
- Simple method
- May be inaccurate in some regions of the patient
- Only one outline for all SPECT slices

B. Line source placed around the patient
- Takes into account the curvature of the patient
- Gives only one outline

C. Compton scatter acquisition
- Finds the outline from a reconstructed Compton image e g by thresholding methods
- Produces matched outlines to SPECT images
- Accuracy may depend on source distribution

D. Transmission measurements
- Produce matched outlines to SPECT images
- Produce also attenuation maps
- May require a separate SPECT study

Tomography with gamma camera

Some scatter correction methods

A. Effective attenuation coefficient (Larsson, Acta Radiol, 1980)

B. Offset energy window (Koral, Nucl Instr Meth, 1985)

C. Deconvolution by Fourier technique (Floyd, J Nucl Med, 1985)

D. Convolution - subtraction methods

1D convolution (y) Axelsson, J Nucl Med, 1984)
2D convolution (x,y) (Msaki, J Nucl Med, 1989)
2D convolution (y,z) (Ljungberg, J Nucl Med, 1990)

E. Multiple energy window methods

Compton window method (Jaszsak, J Nucl Med, 1984)
Dual photopeak window method (King, J Nucl Med, 1992)
Three window method (Ogawa, IEEE Trans Med Imag, 1991)
Channel-ratio method (Pretorius, J Nucl Med, 1993)
Energy spectra analysis (Koral, J Nucl Med, 1988)

What is STEP ?

- Simultaneous
- Transmission
- Emission
- Protocol

What Does STEP Consist Of?

- A set of fan beam collimators
- A transmission line source and a source holder
- Table offset
- Iterative reconstruction software

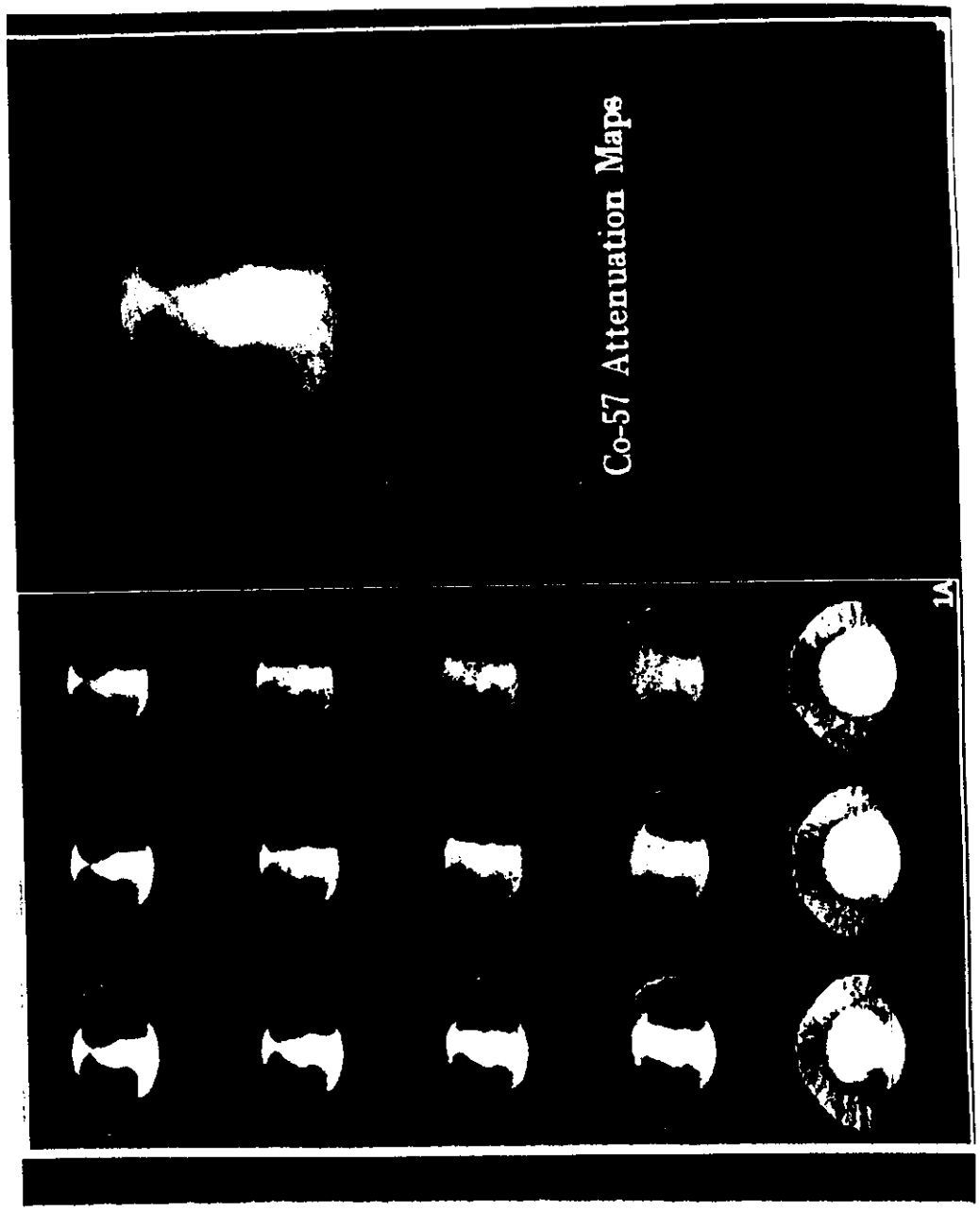

49 y.o. male with end stage renal disease. Conventional images demonstrate decreased activity in the inferior wall. The STEP study was read as normal. Cardiac cath confirmed the STEP results.

Quantification of uptake

		%
Gamma camera	AP + PA :	± 15-20
SPECT		± 10-15
PET		± 5-10

Cylindrical gamma camera using

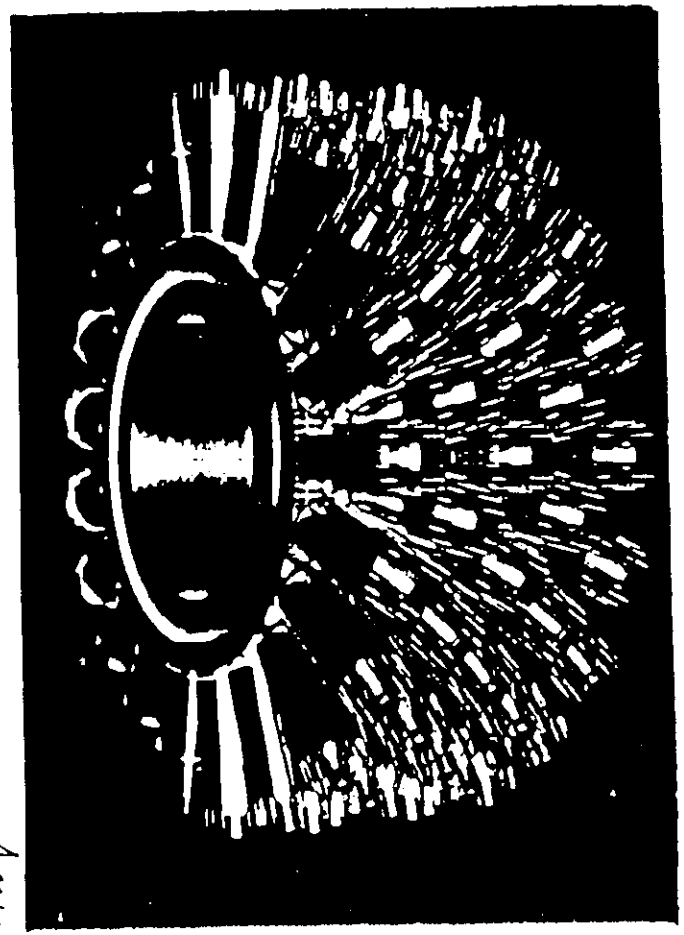

Fig 1. The detector geometry visualized in a SDRC MCAD system.

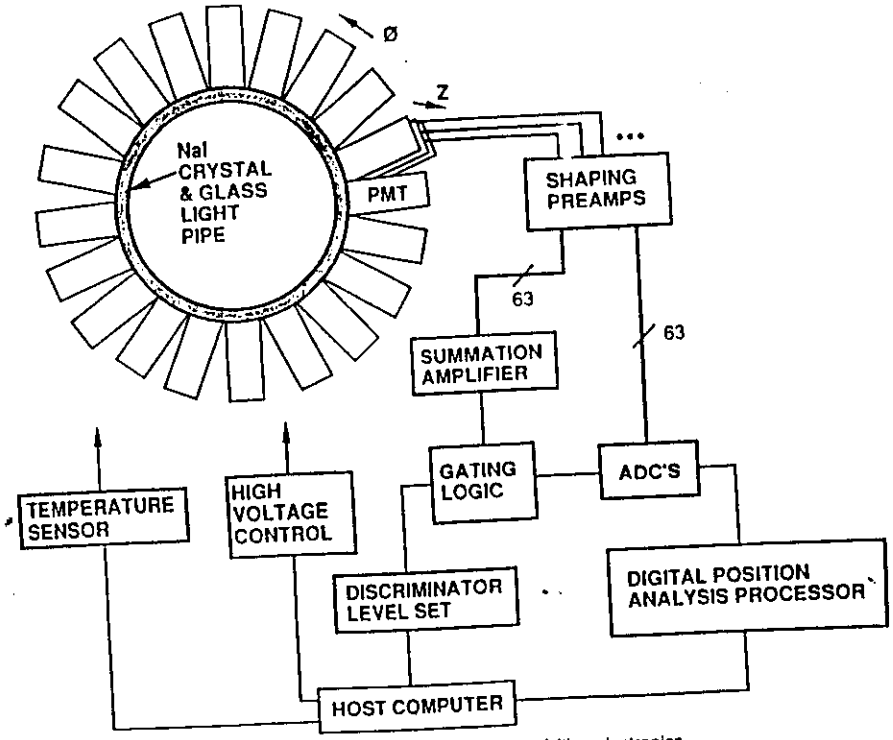

Figure 2. Block diagram of camera data acquisition electronics.

independently adjustable by the computer. These are set to reduce unnecessary deadtime from acquisition of events having improper energies, but within the DPAP a more accurate digital energy window is employed for the final discrimination.

Each PM is separately digitized, and this allows the computer to directly monitor the gains of the PM. The gains are measured in a procedure employing a special calibration collimator and a uniform line source. A history of the gain measurements of each PM is stored by the computer, to provide a record of performance of the system.

One of the more significant features of ASPECT is the monitoring of the temperature of the photomultipliers. PM gain dependence on temperature is a source of system drifts in all cameras, and in a digital camera is the major source. PM gains have a large temperature coefficient that averages about -0.3/°C, but which is different for each PM, and can vary from 0 to -0.6 %/°C. As as example of the errors that can arise, a drift in the gain of one PM over a temperature change of just 1.5°C can more than double the nonlinearity errors, for positions near the offending PM, from their values following calibration. Our system stores the previously calibrated gain temperature coefficients for each PM and uses this to calculate the current PM gain based upon the current temperature and the PM gain and temperature measured during the gain calibration procedure. The PM gains at the time of the image acquisition are then loaded into the DPAP and used in the position algorithms. This helps preserve the accuracy of the PM gain and linearity correction calibrations over time.

Digital Position Analysis

ASPECT is a true digital camera. Signals from each PM are digitized, and all scintillation-event position determinations are calculated digitally. A benefit of this approach, as opposed to the standard analog SPEC cameras, is that the position analysis algorithm can be made more sophisticated. Additional major benefits of computer control and monitoring of signals back to the detector level enables the development of automated diagnostic, quality control, and calibration procedures

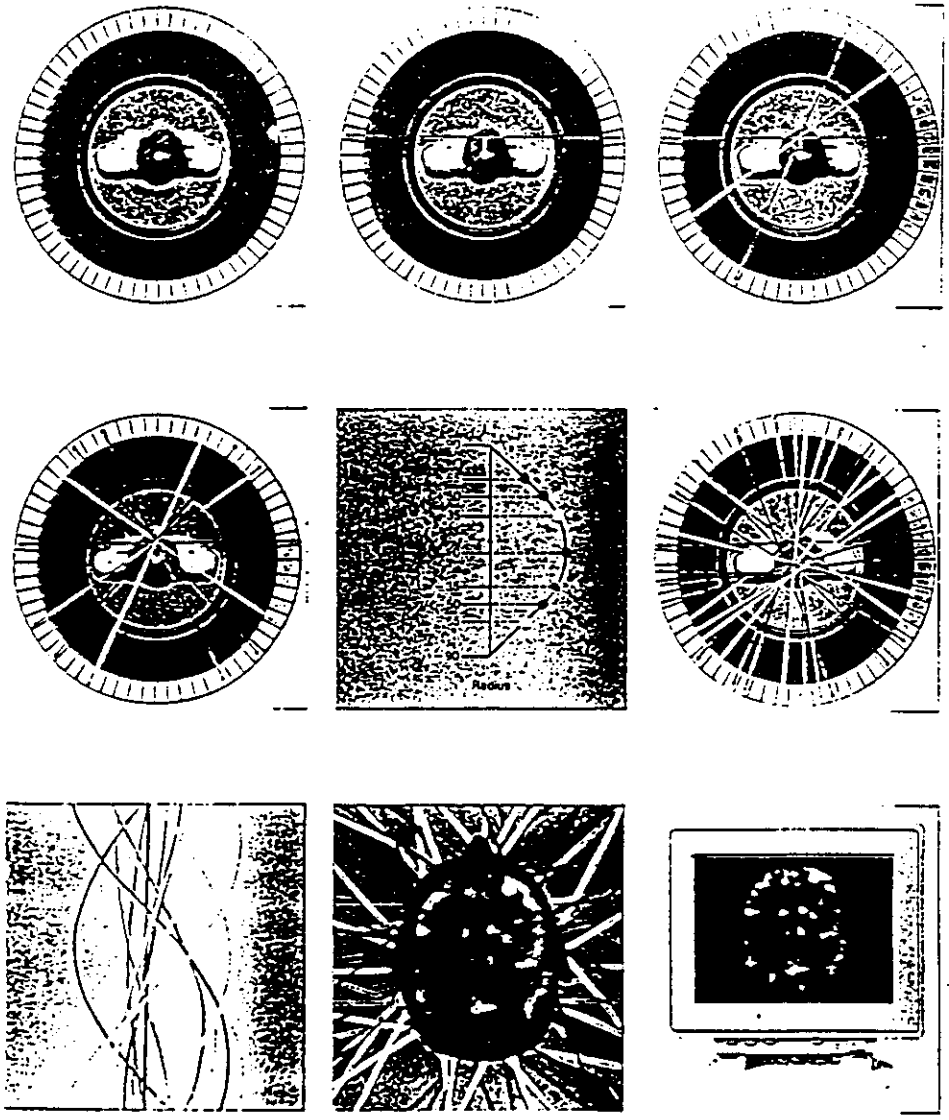

The PET-method

Artificially created isotopes of carbon, nitrogen, oxygen and fluorine are very short-lived and decay by positron emission. These radionuclides can be substituted for corresponding normal atoms in organic substances.

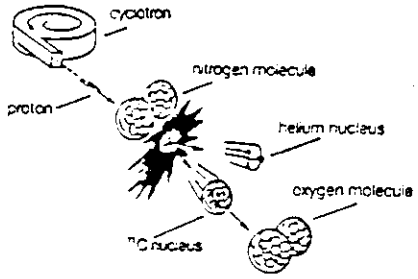

CREATING RADIONUCLIDES

Protons are accelerated in a cyclotron. The high-energy beam of protons is aimed at a mixture of nitrogen and oxygen gas, and splits nitrogen into carbon and helium nuclides. The carbon radionuclide combines with oxygen to give labelled carbon dioxide that is used as a basic component for building other labelled molecules.

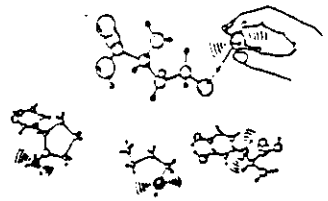

SYNTHESIZING RADIO-TRACERS

The radionuclides are short-lived (2–110 minutes), and the work of building tracer molecules must be done quickly. Special methods are used to configure and assemble molecular parts into PET tracer substances.

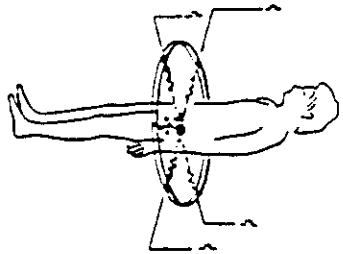

TELL-TALE MOLECULES

After being administered to the patient the decay of the radionuclides is registered. The labelled molecules can be localized in the body with millimeter precision.

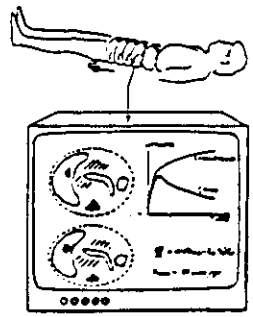

MAPS IN TIME AND SPACE

The computer makes tomographic images from the PET data. The pictures reveal the biological functions of the labelled substance and allow quantitative measurements of drug uptake and kinetics.

PET studies call for well-organized tracer production and full synchronization at all stages from cyclotron to patient. The PET examination usually takes less than 1 hour. Radiation doses are negligible, and repeated examinations can be performed on the same patient.

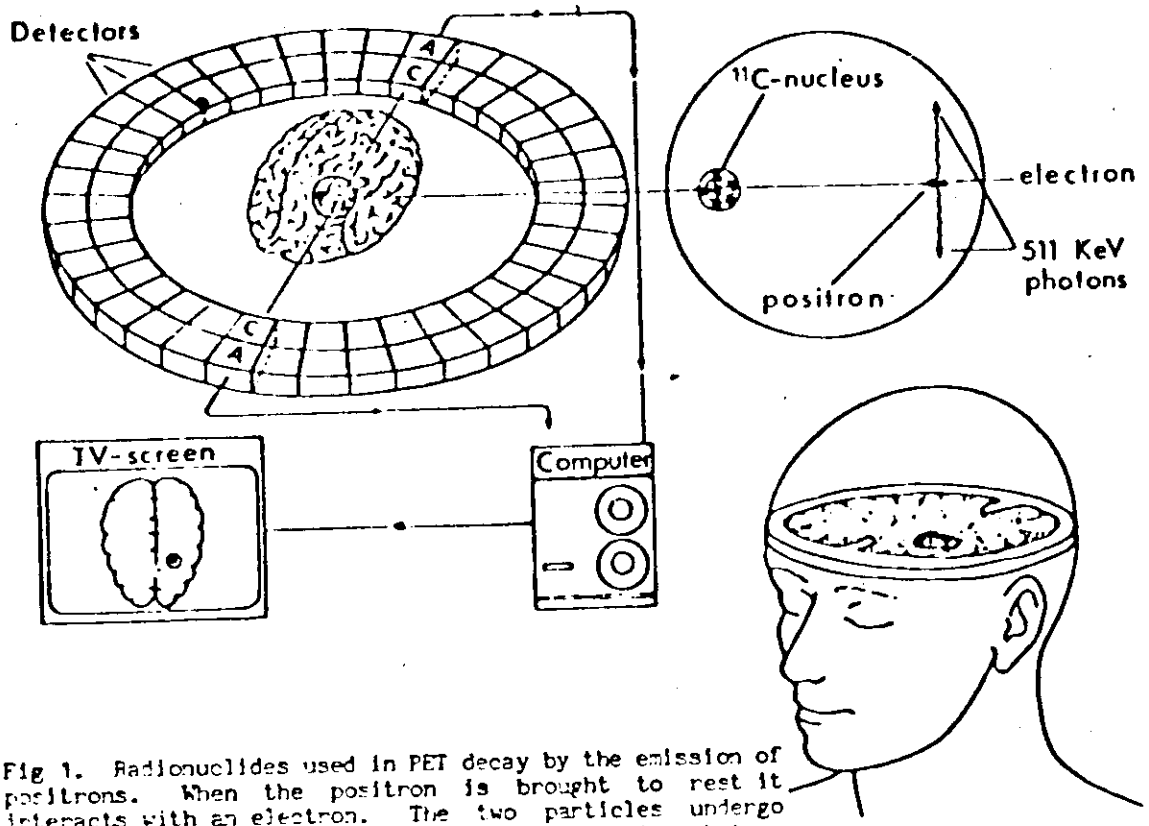

Fig 1. Radionuclides used in PET decay by the emission of positrons. When the positron is brought to rest it interacts with an electron. The two particles undergo annihilation and are converted to annihilation photons travelling 180° from each other. The annihilation photons can be detected with a coincidence system.

Some important positron emitters are C-11, O-15, N-13, F-18, Rb-82, Ga-68, Cu-64 and Kr-77. Due to their short half-lives, C-11 (t 1/2 =20.34 min), O-15 (t 1/2= 2.04 min), N-13 (t 1/2 =9.98 min) and F-18 (t 1/2 =110 min) are most conveniently produced by using dedicated in-house cyclotrons. These isotopes are suitable for labelling biologically interesting substances without significantly altering their biological properties.

Table 1: Properties of potential scintillation detectors for positron computed tomography.

	$Bi_4Ge_3O_{12}$	NaI(Tl)	CsF	BaF_2	Gd_3Si_5O(Ce)
Effective atomic number	74	50	53	54	59
Density (g/cm3)	7.13	3.67	4.64	4.89	6.71
Decay constant (ns)	300	230	2.5	0.8/620	60
Light yield (photons/Mev)	4800	40000	2500	2000/6500	6400
Emission wave-length (nm)	480	410	390	225/310	430
Index of refraction	2.15	1.85	1.48	1.57/1.55	1.9
Energy resolution at 511 keV (FWHM %)	11	9	25	13	14
Hygroscopic	no	yes	yes	little	no

Radiopharmaceuticals for nuclear medicine

Tracer + Radionuclide

- the specific metabolism
- simple labelling
- stabel after labelling
- high target/non-target ratio

Radionuclide

- no particle emission
- short half-life
- good photon-energy
- easy to produce

Radionuclide production

- reactors
- accelerators (cyclotrons)
- (generators)

Radionuclide labelling

I Isotopic

Example:

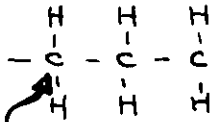

stable carbon atom C-12 exchanged with C-14

II Non-isotopic

Examples

a)

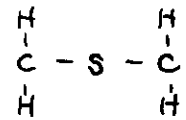

S is exchanged with Se-75

b)

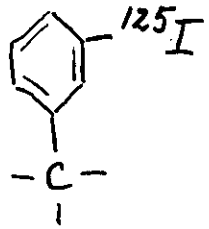

I-125 is put on the molecule

c) Iodination of proteins

Chemical synthesis

^{14}C: start with $^{14}CO_2$, then several steps

^{3}H: precursors + ^{3}H-gas or water

Biosynthesis ("Isotope farming")

Microorganisms + $^{14}CO_2$

Enzymatic synthesis

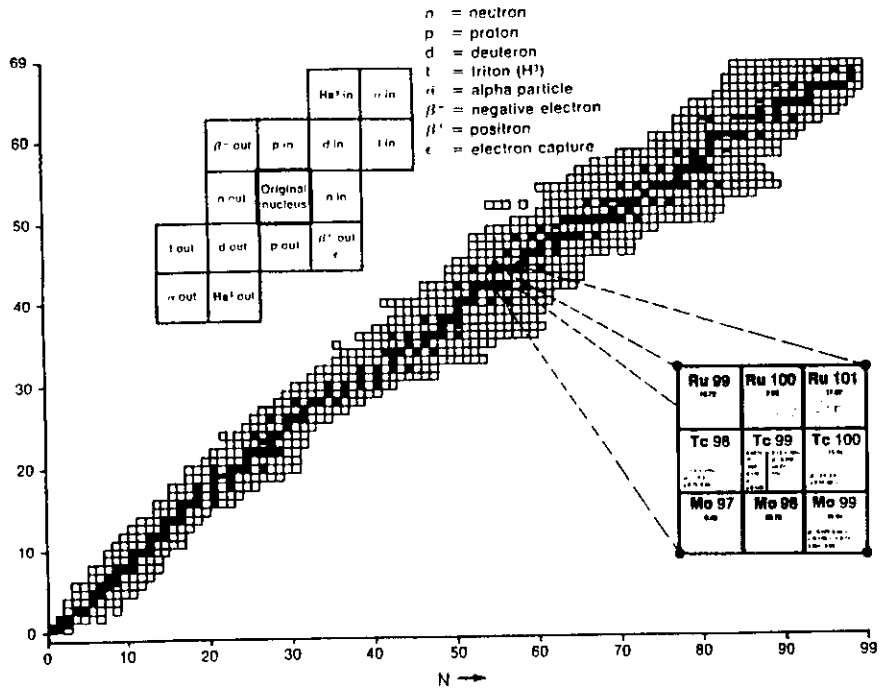

Fig. 4-11. Chart of nuclides (incomplete) showing enlargement of section surrounding ^{99}Tc. Student can refer to large wall charts for detailed information on all known nuclides.

TABLE I
BP radionuclides

Radionuclide	$T_{1/2}$	Most prominent gamma photons (MeV)		Radionuclidic impurities
P-32	14.3d	β_{max} = 1.71		none listed
Cr-51	27.7d	0.320		none listed
Co-57	271d	0.122		Co-60
^{51}Cr	70.8d	0.511, 0.811		Co-60
Fe-59	44.6d	1.10, 1.29		none listed
				Fe-55 not detected
^{67}Ga	3.26d	0.093, 0.185, 0.30		^{66}Ga
^{75}Se	118.5d	0.136, 0.265		none listed
^{99}Tc^{m}	6.02h	0.140		^{99}Mo, ^{131}I, ^{103}Ru, ^{89}Sr, ^{90}Sr
^{125}I	60.1d	0.027		^{126}I
				(13.0d, 0.388, 0.666 MeV)
^{131}I	8.04d	0.365		none listed
^{133}Xe	5.29d	0.081, 0.03-0.035		^{131}Xe^{m}
				(2.19 d, 0.233 MeV)
^{198}Au	2.70d	0.412		^{199}Au
				(0.158 MeV)
Other radionuclides				
^{111}In	2.8d	0.173, 0.247		
^{113}In^{m}	104m	0.390		
^{123}I	13h	0.027, 0.160		
^{201}Ti	73h	0.068, 0.083		

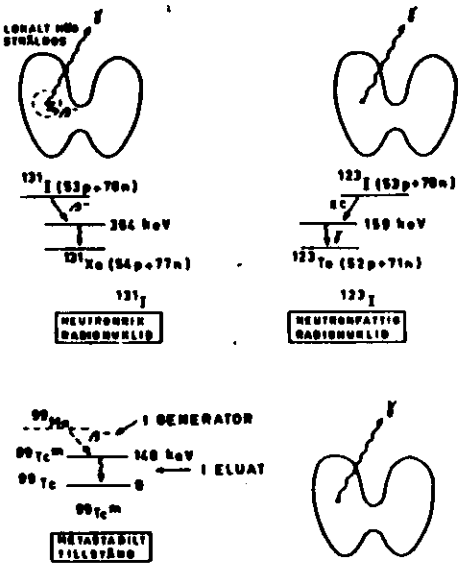

Figur 1. Den för diagnostik med yttre detektorer användbara strålningen utgörs av fotonstrålning, dvs gammastrålning eller karakteristisk röntgenstrålning. Eftersom β⁻-strålning är svår att detektera utanför kroppen kommer den bara att öka patientbestrålningen. Detta är en fördel vid terapi med radioaktiva lösningar men en stor nackdel vid diagnostisk användning. Neutronrika radionuklider sönderfaller oftast via β⁻-sönderfall (ex ^{131}I) medan neutronfattiga sådana kan uppnå stabilitet genom att fånga in en banelektron i härnan (EC = Electron capture, ex ^{123}I). $^{99}Tc^{m}$ är en anhalt, ett metastabilt tillstånd med 6 h halveringstid, i sönderfallet av den neutronrika ^{99}Mo-härnan. (p = proton, n = neutron)

Tabell 1. Strålningsfysikaliska data för några av de inom nuklearmedicinen mest använda radionukliderna

Radionuklid						
Namn	*Kemisk symbol*	*Produktionssätt*[*]	*Reaktor*	*Accelerator*	*Fysikalisk halveringstid*	*Dominerande fotonenergi, keV*
Teknetium-99m	$^{99}Tc^{m}$	^{235}U (n, fission) $^{99}Mo \rightarrow ^{99}Tc^{m}$ ^{98}Mo (n, γ) $^{99}Mo \rightarrow ^{99}Tc^{m}$	X X		6,03 timmar	140
Xenon-133	^{133}Xe	^{235}U (n, fission) ^{133}Xe	X		5,31 dygn	81
Jod-131	^{131}I	^{130}Te (n, γ) $^{131}Te \rightarrow ^{131}I$	X		8,06 dygn	364
Jod-125	^{125}I	^{124}Xe (n, γ) $^{125}Xe \rightarrow ^{125}I$	X		60,2 dygn	28
Jod-123	^{123}I	^{127}I (p, 5n) $^{123}Xe \rightarrow ^{123}I$		X	13,0 timmar	159
Tallium-201	^{201}Tl	^{203}Tl (p, 3n) $^{201}Pb \rightarrow ^{201}Tl$		X	3,1 dygn	69–83
Krom-51	^{51}Cr	^{50}Cr (n, γ) ^{51}Cr	X		27,7 dygn	320
Kobolt-57	^{57}Co	^{60}Ni (p, α) ^{57}Co		X	250 dygn	122
Indium-111	^{111}In	^{112}Cd (p, 2n) ^{111}In		X	2,81 dygn	172, 247
Indium-113m	$^{113}In^{m}$	^{113}Sn (n, γ) $^{113}Sn \rightarrow ^{113}In^{m}$	X		1,67 timmar	247
Järn-59	^{59}Fe	^{58}Fe (n, γ) ^{59}Fe	X		45,0 dygn	1099, 1292
Väte-3 (tritium)	^{3}H	^{6}Li (n, α) ^{3}H	X		12,3 år	–
Kol-14	^{14}C	^{14}N (n, p) ^{14}C	X		5730 år	–
Kol-11	^{11}C	^{10}B (d, n) ^{11}C m fl		X	20,4 minuter	511
Kväve-13	^{13}N	^{10}B (α, n) ^{13}N m fl		X	9,96 minuter	511
Syre-15	^{15}O	^{14}N (d, n) ^{15}O m fl		X	2,05 minuter	511
Fluor-18	^{18}F	^{20}Ne (d, α) ^{18}F m fl		X	1,83 timmar	511

[*] A(a, b) B = A + a → B + b

$$^{99}Mo \xrightarrow[\beta^-]{T_{1/2} = 66,7\ \text{tim.}} {}^{99}Tc^{m} \xrightarrow[\gamma]{T_{1/2} = 6,03\ \text{tim.}} {}^{99}Tc$$

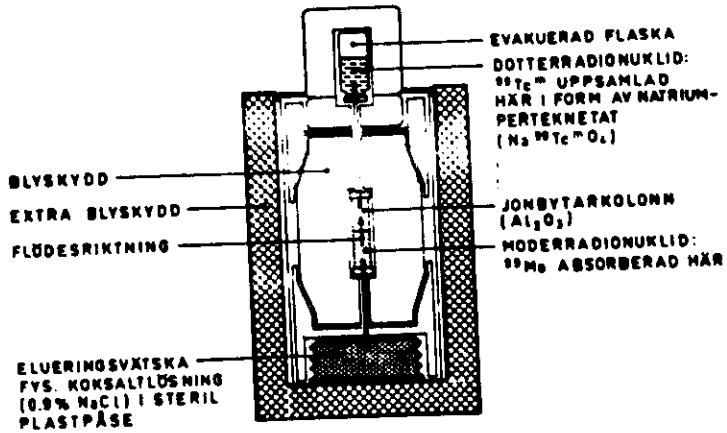

Figur 2. Genomskärning av en $^{99}Tc^{m}$-generator. Moderradionukliden ^{99}Mo produceras antingen genom neutronbestrålning av ^{235}U och efterföljande kemisk separation av Mo från fissionsproduktblandingen eller via neutronbestrålning (aktivering) av naturligt molybden, som till 23,8% utgörs av ^{98}Mo. ^{99}Mo fästes på en jonbrytare, som håller kvar moderradionukliden medan dotterprodukten $^{99}Tc^{m}$ kan tvättas ur med fysiologisk koksaltlösning.

TABLE 1-1. CHEMICAL AND PHYSICAL FORMS OF RADIOPHARMACEUTICALS

Elemental	^{133}Xe	^{127}Xe	^{81m}Kr
Simple ions	$^{131}I^-$	$^{99m}TcO_4^-$	$^{111}In^{3+}$
Labeled small molecules	O-iodohippuric acid-I-131 (covalently bonded)		^{111}In-diethylene triamine penta acetic acid (In-111-DTPA) (complexation)
Labeled macromolecules	Proteins (I-125-human serum albumin)		
Labeled particles	Colloids (Tc-99m-sulfur colloid) Albumin aggregates and microspheres (Tc-99m)		
Labeled cells	Erythrocytes (Cr-51, Tc-99m) Leukocytes (In-111) Platelets (In-111)		

MECHANISMS OF LOCALISATION OF RADIOPHARMACEUTICALS

TABLE 1
Mechanisms of localisation of radiotracers

Substrate nonspecific:
1. Diffusion:
   a) Technetium-99m pertechnetate for Brain imaging.
   b) Xenon-133 and Krypton-81m for lung ventilation.
2. Isotope dilution:
   a) Iodine-125 Human albumin for plasma volume.
   b) Chromium-51 erythrocytes for red cell mass.
3. Capillary blockade and cell sequestration:
   a) Technetium-99m macroaggregated albumin for regional lung perfusion studies.
   b) Technetium-99m heat damaged erythrocytes for splenic sequestration.
4. Phagocytosis:
   a) Technetium 99m tin colloid for liver scanning.

Substrate specific:
1. Metabolic pathway [isotopic substitution]:
   a) Carbon-11 glucose for regional brain studies.
   b) Iodine-123 iodide for thyroid studies.
2. Metabolic pathway [non-isotopic substitution]:
   a) Iodine-123 iodoheptadecanoic acid.
3. Metabolic trapping:
   a) Technetium-99m pertechnetate for thyroid studies.
   b) Fluorine-18 2-deoxy-2-fluoro-D-glucose for regional brain studies.
4. Enzyme substrate:
   a) Selenium-75 substituted norcholesterol for adrenal scanning.
   b) Selenomethionine for pancreas scanning.
5. Receptor binding:
   a) Alpha-1 adrenoreceptor antagonists.
6. Antibodies:
   a) Anti CEA antibodies for tumour imaging.
   b) Antithrombocyte antibodies for thrombus detection.
   c) Antimyosin antibodies for myocardial studies.

Bone scintigraphy

$^{99}Tc^{m}$ labelled radiopharmaceuticals

- albumine
- albumine aggregates (particles) 10-40 µm, 0.5 µm, 0.05 µm
- sulfur colloid 0,5µm
- DTPA (diethylene-triamine-penta acetic acid)
- GHA (glucoheptonic acid)
- DMSA (dimercaptosuccinic acid)
- IDA (iminodiacetic acid)
  - HIDA
  - DISIDA
  - IODIDA
- phosphates
  - MDP (methyldiphosphonate)
  - DPD (dicarboxy diphosphonate)
- HMPAO (propyleneamineoxime)
- aerosols
  - Liquid droplets
  - carbon particles
- RBC
- MAG 3
- MIBI (methyloxyisobutyl isonitrile)
- MoB

^{125}I, ^{131}I, ^{123}I-Labelled radiopharmaceuticals

- albumine
- fibrinogene
- ortho iodo hippurate
- iodo methyl nor colesterol
- MIBG (metaiodo benzylguanidine)

Other radiopharmaceuticals

- ^{201}Tl
- ^{133}Xe
- ^{75}Se norcolesterol
  - bile acid (SeHCAT)
- ^{51}Cr chromat
  - EDTA

^{111}In oxine
- leucocytes
- platelets

^{131}I MoB

^{111}In octreotide

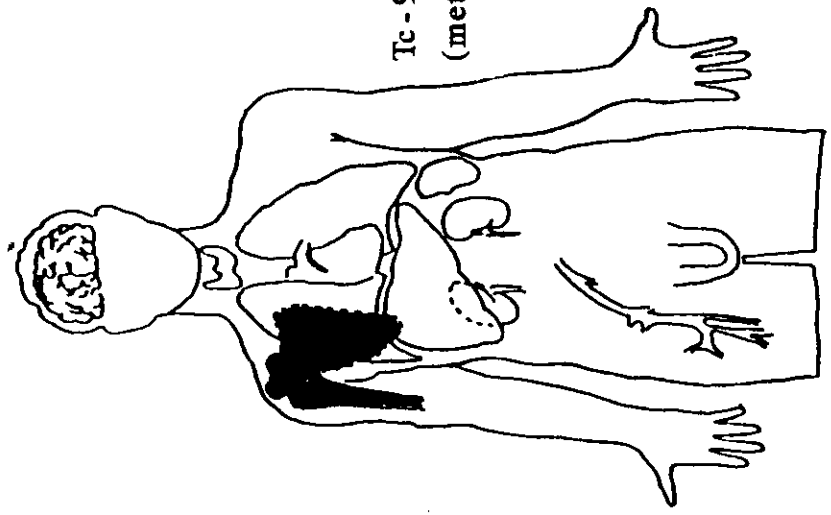

Tc-99m MDP
(methylenediphosphonate)

Kidneys

Renal clearance (GFR)

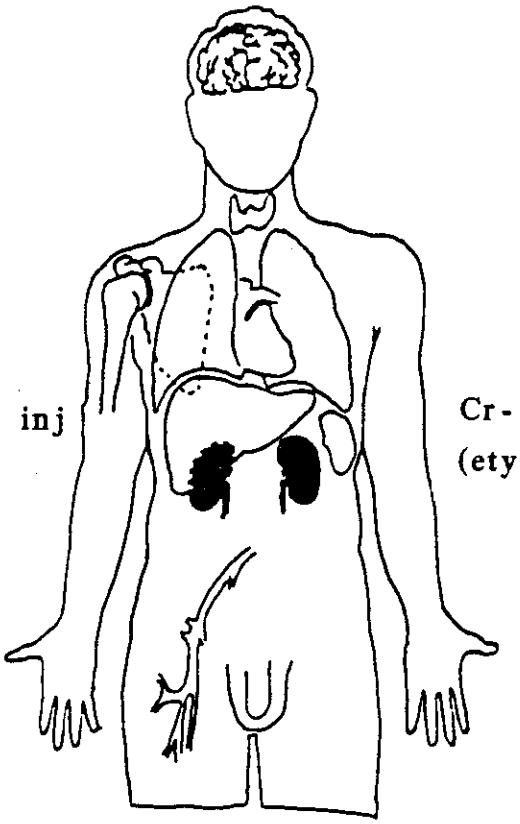

Blood samples 3-4 h after inj

Cr-51 EDTA
(etylenediaminetetraacetate)

Kidneys
Gamma camera imaging and renography

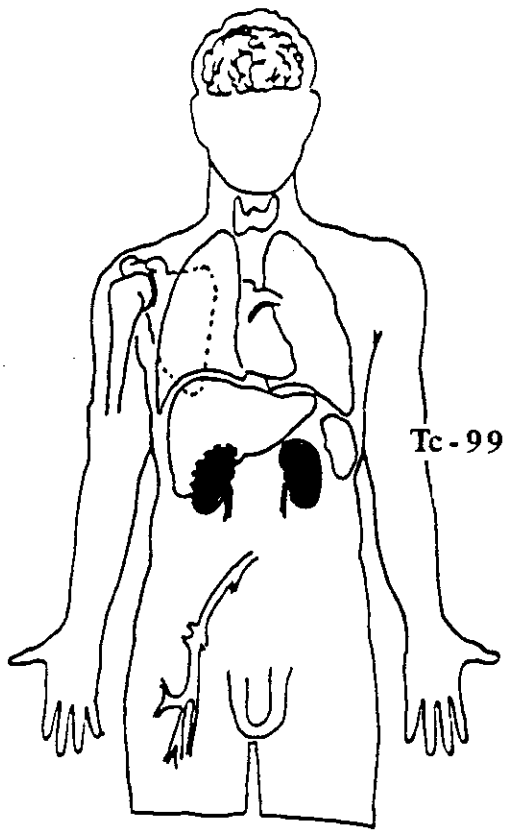

Tc-99m MAG3, -DTPA, -DM

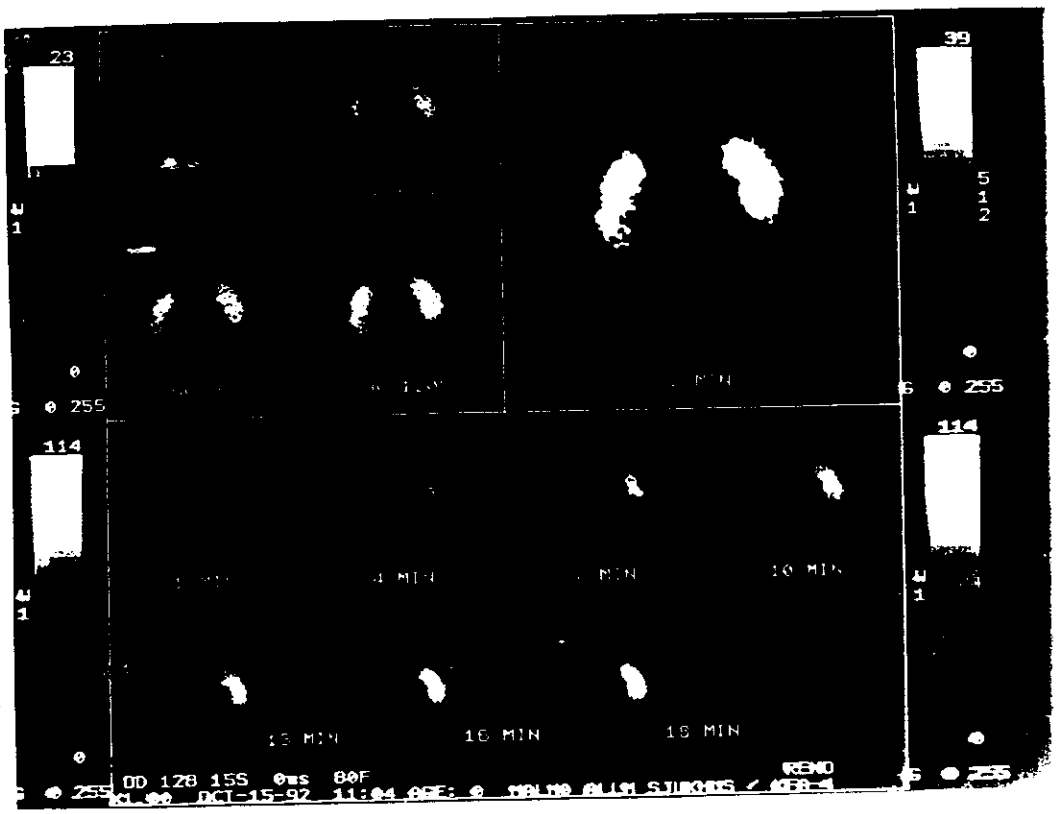
23
39
114
114
4 MIN
10 MIN
16 MIN
18 MIN
0 255
OD 128 15S 0ms 80F
X1.00 OCT-15-92 11:04 AGE: 0 MALMÖ ALLM SJUKHUS / KFA-4
RENO

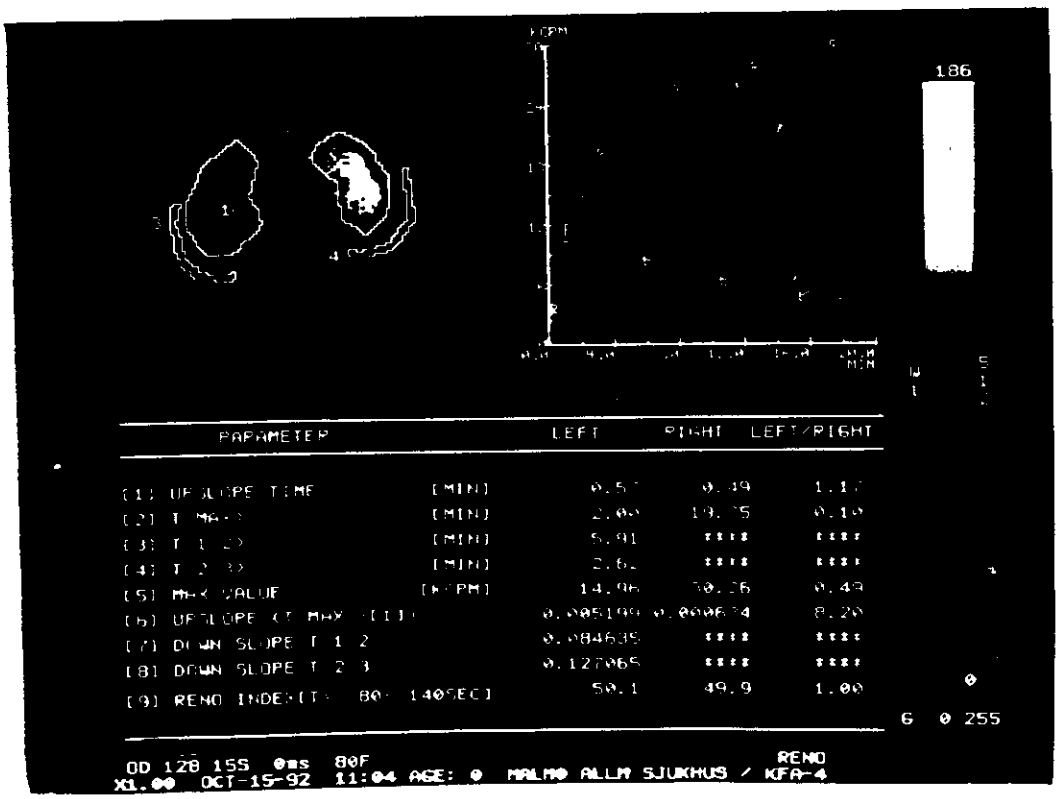
186
PARAMETER LEFT RIGHT LEFT/RIGHT
[1] UP SLOPE TIME [MIN] 0.57 0.49 1.17
[2] T MAX [MIN] 2.04 10.75 0.19
[3] T 1 2 [MIN] 5.91 **** ****
[4] T 2 3 [MIN] 2.61 **** ****
[5] MAX VALUE [K-PM] 14.96 30.26 0.49
[6] UP SLOPE (T MAX - [1]) 0.005199 0.006634 0.78
[7] DOWN SLOPE T 1 2 0.004635 **** ****
[8] DOWN SLOPE T 2 3 0.127965 **** ****
[9] RENO INDEX (T= 80- 140SEC] 50.1 49.9 1.00
0 255
OD 128 15S 0ms 80F
X1.00 OCT-15-92 11:04 AGE: 0 MALMÖ ALLM SJUKHUS / KFA-4
RENO

Thyroid

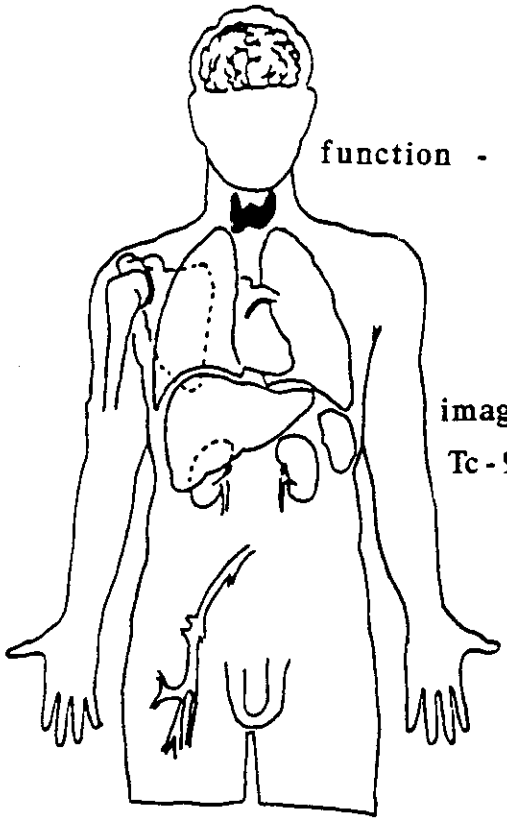

Fig. 4-13. Two examples are analog tracers with similar biodistributions resulting from similar physical chemical characteristics of ionic size and charge. In their initial biodistributions, pertechnetate ions mimic iodide ions, and thallous ions mimic potassium ions.

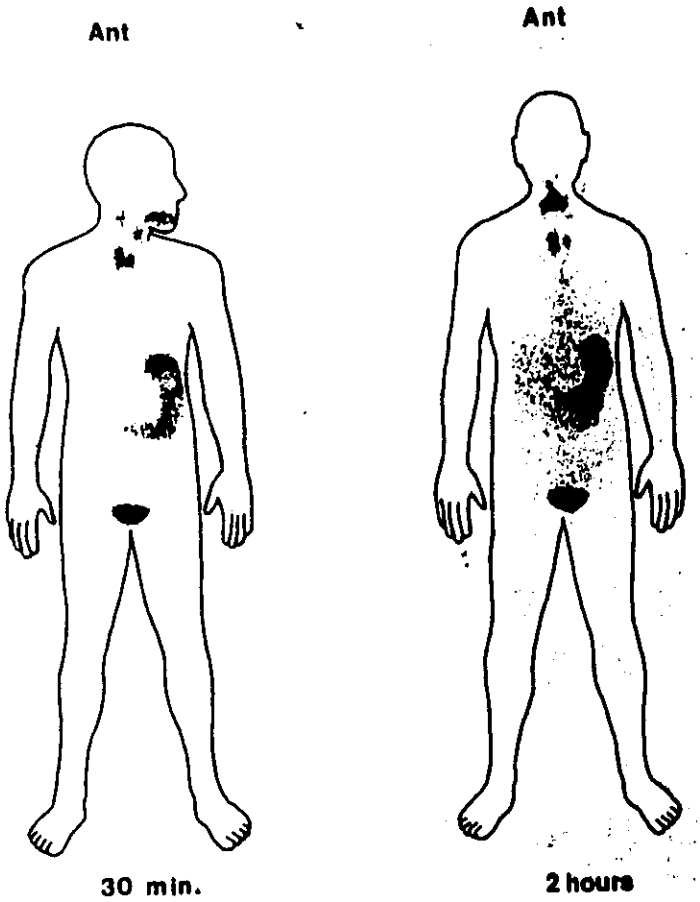

Figure 1–4. Whole-body distribution of ^{99m}Tc sodium pertechnetate without perchlorate blocking. Activity is seen in the thyroid gland, salivary glands, mouth, stomach, and bladder.

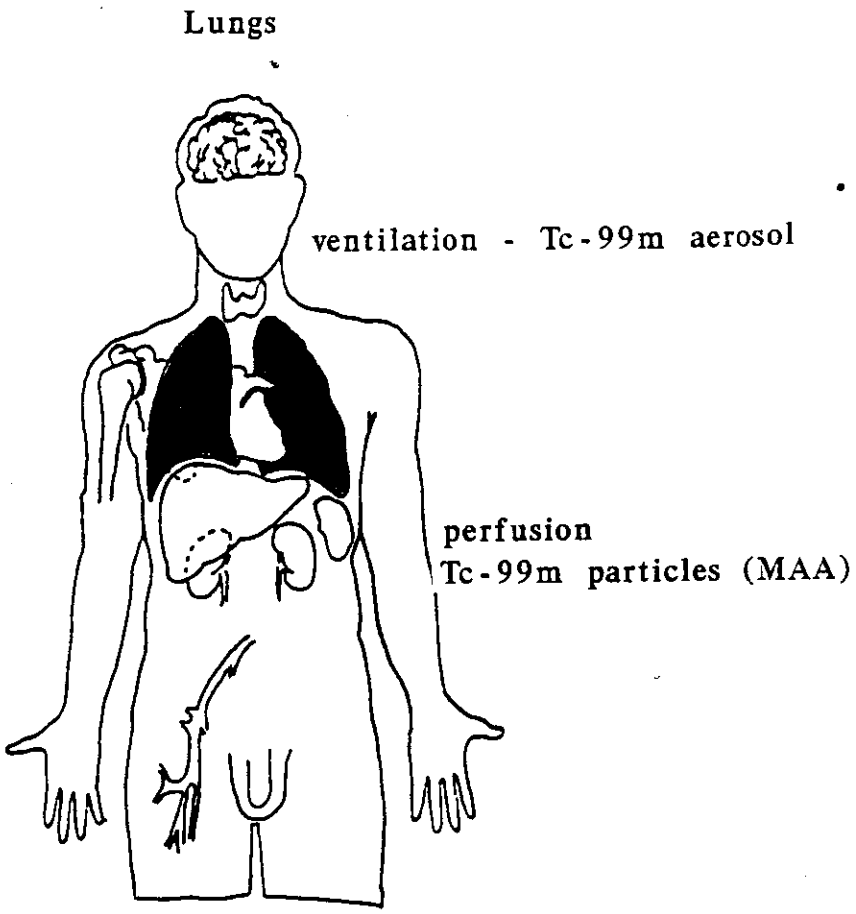

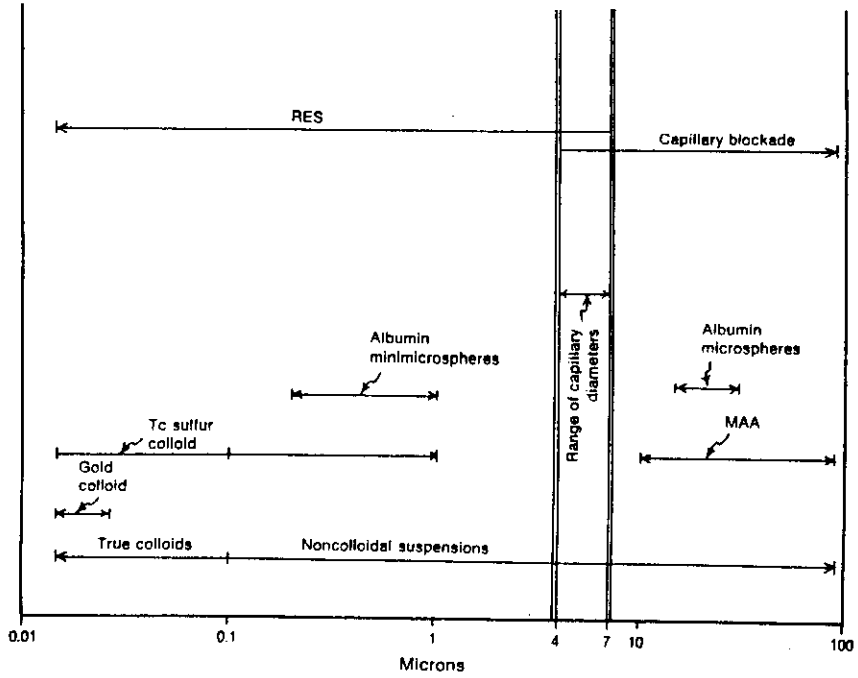

Fig. 4-7. Particles are removed from bloodstream primarily by RES or by capillary blockade. This drawing allows reader to compare size ranges for different particulate radiopharmaceuticals to size of capillary and to colloids.

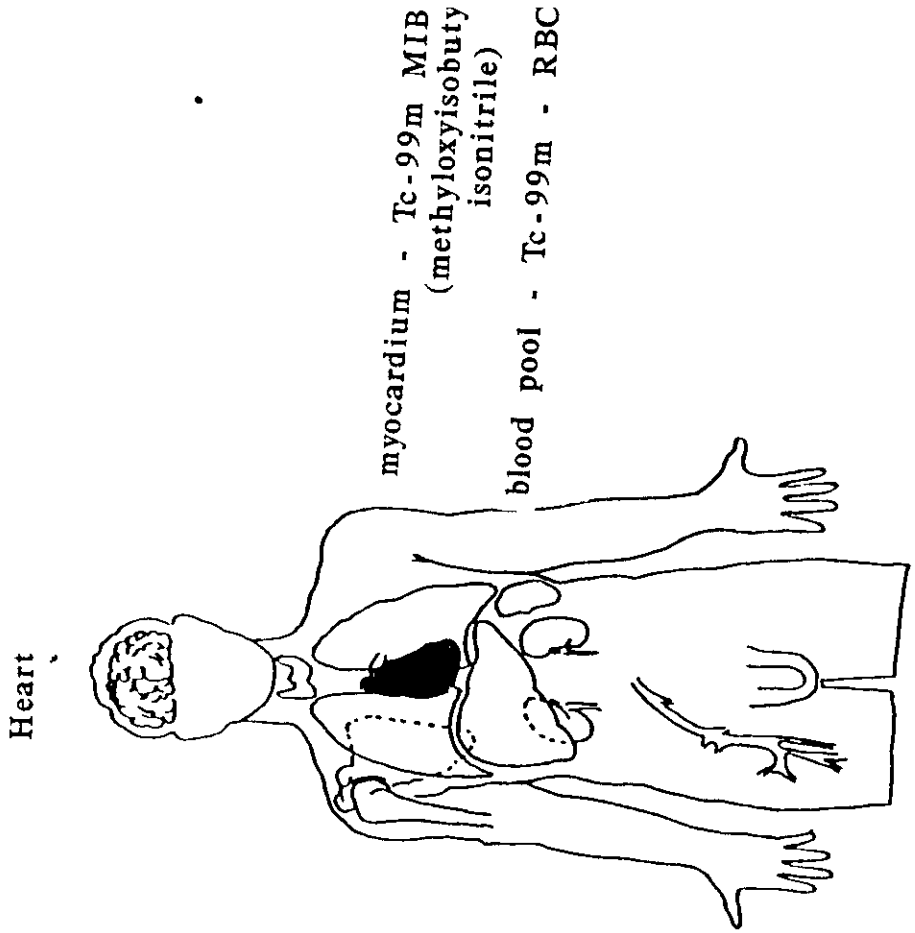

Liver, spleen, bone-marrow

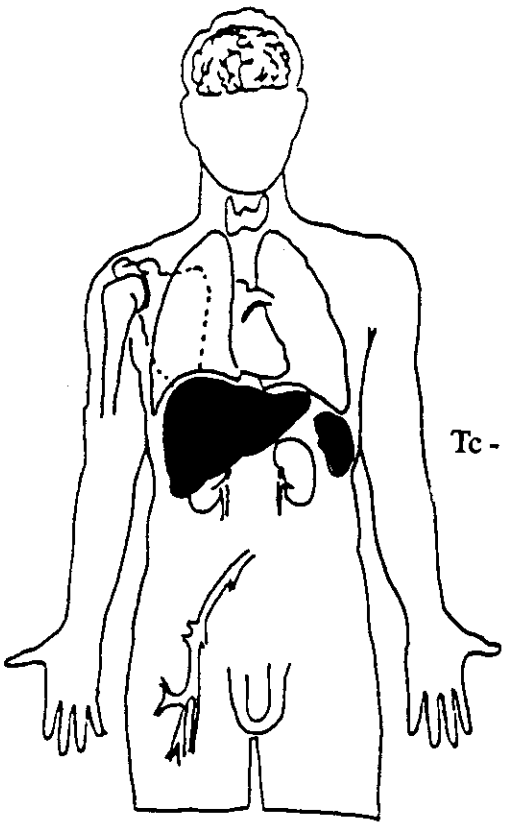

Tc-99m colloid

Brain scintigraphy

Momentary cerebral blood flow

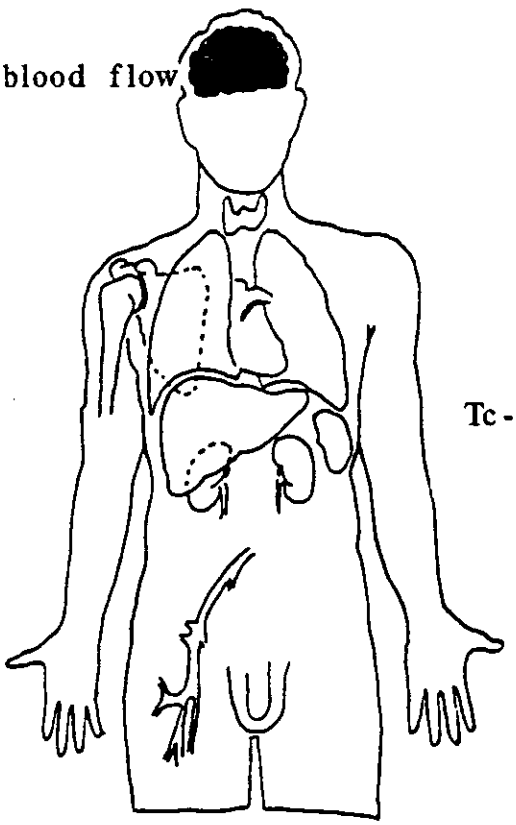

Tc-99m HM-PAO

(hexamethylpropyle
amineoxine

Gall-bladder

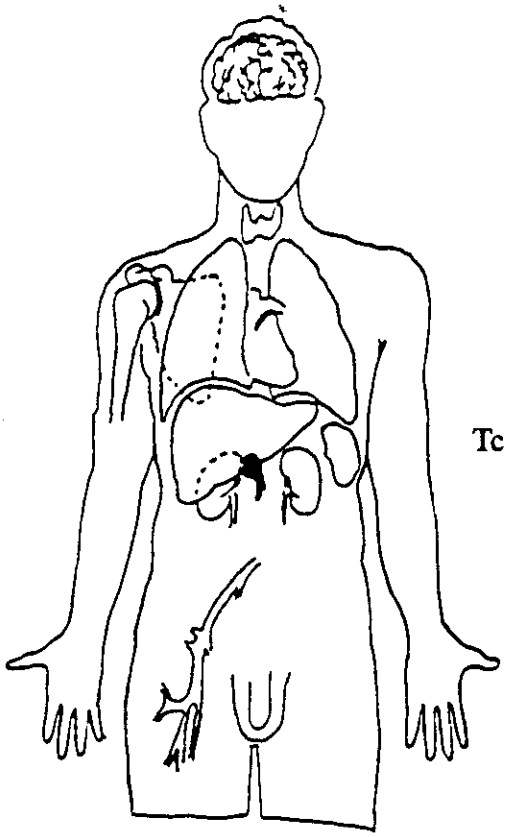

Tc-99m HIDA

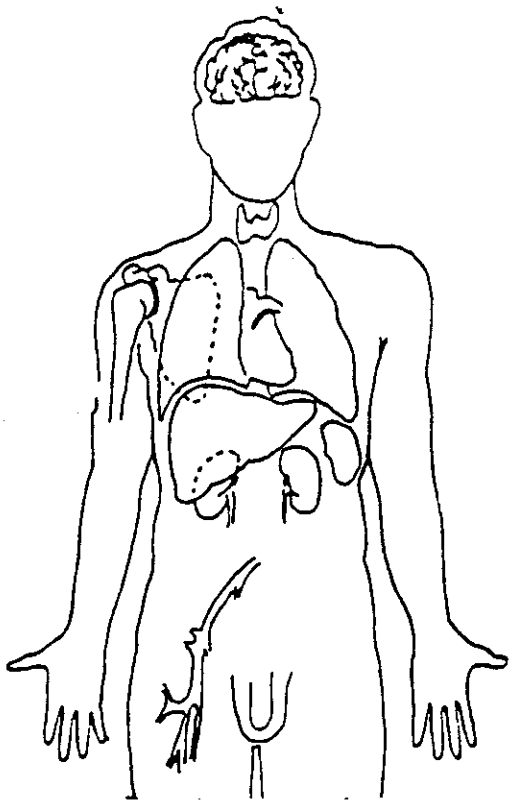

Inflamation, abscesses - In-111 leukocytes
Circulation - Tl-201, Tc-99m RBC
Thrombi - In-111 platelets

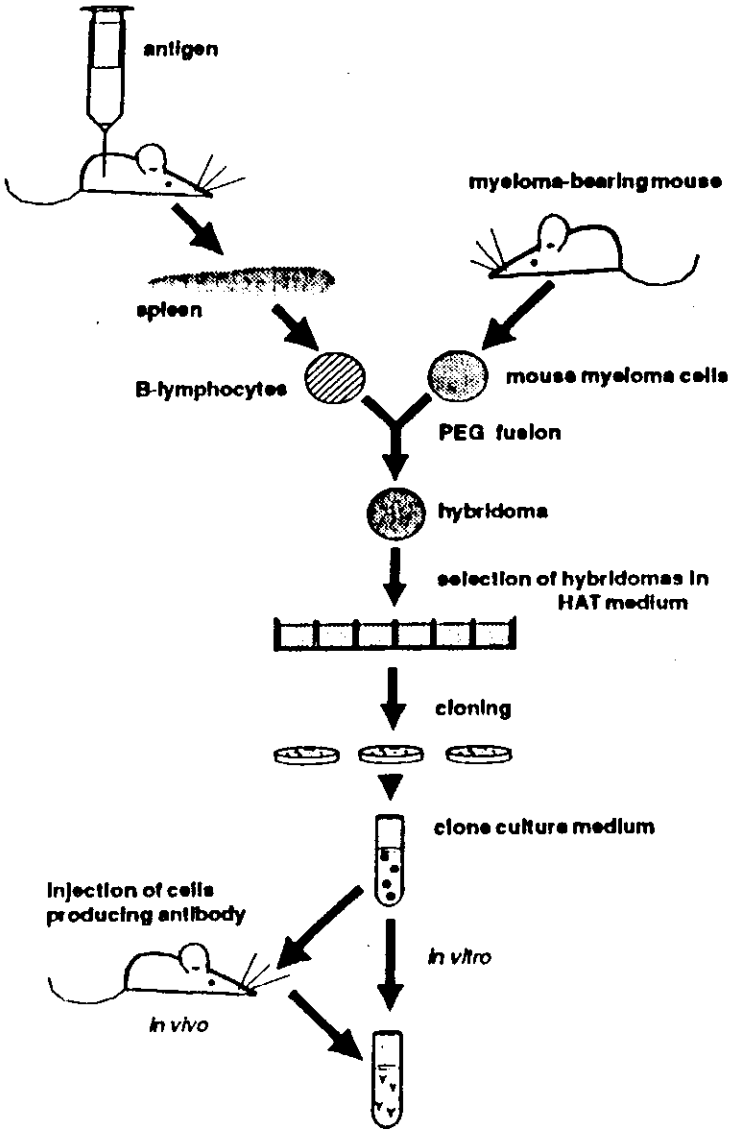

Figure 2. Schematic representation of the production of monoclonal antibodies (Forssell Aronsson 1992b).

Cancer

In-111 octreotide

Radiolabeled monoclonal antibodies
(more specific and new antigens)

FDG PET
Tl-201 ion
Tc-99m MIBI
I-123 MIBG

Characterization with multi-tracer studies

Octreotide - a somatostatin analog

A small peptide

May be labeled with I-131 and I-123
or chelated with In-111

High target-to-background ratios >>
>>small tumors can be visualized
>>potential for therapy

Imaging of somatostatin receptor sites in:
Neuroendocrine tumours
Breast cancers
Non-Hodgkin and Hodgkin lymphomas
Granulomata
Sarcoidosis
mm

Positive I-123 imaging is predictive of therapeutic response with non-labelled octreotide.

Clearance via the gall bladder might obscure some abdominal tumors

SUBSTANCE	TUMOUR/NORMAL TISSUE CONCENTRATION RATIO
Somatostatin - analog	30 - 100
Monoclonal antibody	1 - 10

Therapy with radiopharmaceuticals

	Diagnostics	Therapy	No of pat. 1991
Thyreotoxicosis Thyroid ca	Tc-99m pertechnet I-131 jon	I-131 ion (p.o.)	3 000
Polycytemia		P-32 phosphate (p.o.,i.v.)	280
Bone metastasis (pain)	Tc-99m MDP	Sr-89 ion (i.v.)	230
Joints		Y-90 silicate (i.articul.)	30
Tumours		Y-90 colloid (i.v.,i.t.)	10
	Monocl antib	Monocl antib	
Neuroendocrine tumours	I-123/131 MIBG	I-131 MIBG (i.v.)	4

Has Nuclear Medicine got a Future?

For:

Functional imaging
Whole body imaging

Clinical need
Research potential

Therapy

Improving instrumentation
Improving data processing
Commercial nuclear pharmacy

The third world

Against:

Competetive techniques (MR, CT, US etc)
Closing of reactors
Air transport limitations
Pharmaceutical regulations
Problems with organization